Archives of Toxicology (2019) 93:965–986
https://doi.org/10.1007/s00204-019-02415-8

ORGAN TOXICITY AND MECHANISMS

Sirtuin-1 ameliorates cadmium-induced endoplasmic reticulum stress and pyroptosis through XBP-1s deacetylation in human renal tubular epithelial cells

Xin Chou[1,2] · Fan Ding[1,2] · Xiaoyan Zhang[3,4,5] · Xiaoqiang Ding[3,4,5] · Hui Gao[1,2] · Qing Wu[1,2]

Received: 16 September 2018 / Accepted: 14 February 2019 / Published online: 22 February 2019

Abstract

Cadmium (Cd), an occupational and environmental pollutant, induces nephrotoxicity by primarily damaging renal proximal tubular cells. In this study, we hypothesized that pyroptosis, a caspase-1-dependent inflammatory programmed cell death mechanism, mediates Cd-induced nephrotoxicity. Human proximal tubular epithelial HK-2 cells were treated with 0–10 μM $CdCl_2$ for 48 h. We found that Cd dose-dependently caused cytotoxicity, which correlated with activation of the NLRP3 inflammasome, increases in the expression and secretion of pro-inflammatory cytokines and upregulation of pyroptosis-related genes in HK-2 cells or/and in kidneys of Cd-treated mice. These effects were significantly abrogated by inhibiting caspase-1 activity with inhibitor YVAD or silencing NLRP3 with siRNA in vitro, suggesting that Cd induces caspase-1- and NLRP3-inflammasome-dependent pyroptosis. Moreover, Cd treatment also activated three branches (ATF6, PERK and IRE-1α) of endoplasmic reticulum stress. Selective inhibition of the IRE-1α/XBP-1s branch by a pharmacological inhibitor STF-083010 or by genetic silencing of XBP-1 significantly attenuated Cd-induced NLRP3 inflammasome activation and pyroptosis. Mechanistically, Cd suppressed deacetylase Sirtuin-1 (SIRT-1) protein expression and activity leading to decrease in physical binding with XBP-1s protein, and thus the accumulation of acetylated XBP-1s levels. Activation of SIRT1 using a pharmacological agonist resveratrol or genetic SIRT1 overexpression significantly abolished Cd-induced activation of the IRE-1α/XBP-1s pathway and the NRLP3 inflammasome as well as pyroptosis, which were counteracted by co-overexpression of both SIRT1 and XBP-1s. Collectively, our findings indicate that SIRT1 activity protects against Cd-induced pyroptosis through deacetylating XBP-1s, and thus inhibiting the IRE-1α/XBP-1s pathway in HK-2 cells. These results provide a novel mechanism for Cd-induced nephrotoxicity.

Keywords Cadmium · SIRT1 · ER stress · Pyroptosis · Renal cells

Abbreviations

ATF6	Activating transcription factor 6
Cd	Cadmium
ER	Endoplasmic reticulum
IRE-1α	Inositol-requiring enzyme 1α
NLRP3	Nucleotide-binding oligomerization segment-like receptor family 3 inflammasome
PERK	Protein kinase RNA-like endoplasmic reticulum kinase
XBP-1s	Splice X-box binding protein-1
SIRT1	Sirtuin-1

Electronic supplementary material The online version of this article (https://doi.org/10.1007/s00204-019-02415-8) contains supplementary material, which is available to authorized users.

✉ Qing Wu
qingwu@fudan.edu.cn

[1] School of Public Health, Fudan University, 130 Dong'An Road, P.O. Box 288, Shanghai 200032, China

[2] Key Laboratory of Public Health Safety, Ministry of Education, 130 Dong'An Road, Shanghai 200032, China

[3] Kidney and Dialysis Institute of Shanghai, 136 Medical College Road, Shanghai 200032, China

[4] Kidney and Blood Purification Laboratory of Shanghai, 136 Medical College Road, Shanghai 200032, China

[5] Department of Nephrology, Zhongshan Hospital, Fudan University, 180 Fenglin Road, Shanghai 200032, China

Introduction

Cadmium (Cd), a toxic heavy metal, is ubiquitously found in the environment and exhibits high soil-to-plant transfer rate (Faroon et al. 2012; Satarug 2018). Cd pollution is still a serious public health challenge for many developing countries including China. A recent epidemiological study conducted in Southwest China reported that the means of dietary Cd levels were 113.1, 88.8 and 16.5 μg/kg bw/month in residents of high Cd-polluted, low Cd-polluted and control areas, respectively (Huo et al. 2018). Such levels of dietary Cd are much higher than the provisional tolerable monthly intake (25 μg/kg bw/month) established by the Joint FAO/WHO Expert Committee on Food Additives in 2011 (Huo et al. 2018). Cd exposure can damage multiple organ systems in humans and animals. The kidney is the major target due to the fact that approximately 50% of the total Cd body burden accumulates in this organ (Yang and Shu 2015). The renal toxicity of Cd is primarily characterized by dysfunctions of proximal tubules leading to proteinuria and eventually chronic kidney diseases (Jarup and Akesson 2009). It has been reported that both urinary and blood Cd levels positively correlated with the increased levels of urinary β2 microglobulin and *N*-acetyl-β-D-glucosaminidase (two marker proteins of renal tubular damage) in subjects from Cd polluted areas in China (Chen et al. 2018b; Chen and Zhu 2018; Zhang et al. 2013). Using in vitro culture of human proximal tubular epithelial HK-2 cells, we recently showed that chronic treatment of Cd (1 μM for 12 days) induced endoplasmic reticulum stress, inhibited protein kinase B signaling and altered gap junctional intercellular communication formation, all of which contributed to Cd-induced apoptosis (Ge et al. 2018).

Unlike non-inflammatory apoptosis, pyroptosis is a highly pro-inflammatory programmed cell death and is characterized by caspase-1 dependence, cell membrane destruction and the release of pro-inflammatory intracellular contents (Bergsbaken et al. 2009). Pyroptosis can be induced by both infectious and non-infectious stimuli through the secretion of pathogen-associated molecular patterns (PAMPs) or damage-associated molecular patterns (DAMPs), respectively (Lu et al. 2014). PAMPs or DAMPs then trigger the assembly and activation of nucleotide-binding oligomerization segment-like receptor family 3 (NLRP3) inflammasome. The N-terminal pyrin domain (PYD) of NLRP3 protein serves as a scaffold for the recruitment of nucleate apoptosis-associated speck-like protein containing a caspase recruitment segment (ASC), which then binds to pro-caspase-1 and triggers its auto-activation into cleaved caspase-1 (c-caspase-1) (Lu et al. 2014; Schroder and Tschopp 2010). Activation of caspase-1 leads to proteolytic cleavage of precursor interleukin 1β (pro-IL-1β) and IL-18 (pro-IL-18) into inflammatory mature IL-1β and IL-18, respectively (Fantuzzi and Dinarello 1999). These biologically active inflammatory cytokines IL-1β and IL-18 are then released into extracellular compartments to induce inflammation through cleaved Gasdermin D (GSDMD)-mediated formation of pores on cell membranes (He et al. 2015; Shi et al. 2015). It has been shown that Cd treatment could induce NRLP3 inflammasome-dependent pyroptosis in human umbilical vein endothelial cells (HUVEC) (Chen et al. 2016). However, whether pyroptosis is the potential mechanism of Cd-induced cytotoxicity in renal epithelial cells remains unclear.

Endoplasmic reticulum (ER) is the primary organelle for protein synthesis, processing and secretion (Benham 2012; Ellgaard and Helenius 2003). Impairment of ER function by intracellular or/and extracellular stimuli causes the accumulation of misfolded and unfolded proteins in ER lumen, resulting in ER stress (Hasnain et al. 2012; Ron and Walter 2007). Subsequently, three unfold protein response (UPR) pathways including the inositol-requiring enzyme 1α (IRE-1α) pathway, the protein kinase RNA-like endoplasmic reticulum kinase (PERK) pathway and the activating transcription factor 6 (ATF6) pathway are activated to restore ER homeostasis and promote cell survival (Ron and Walter 2007; Xu et al. 2005). However, prolonged activation of the UPR leads to orchestrated cell death (Schroder 2008). Activation of IRE-1α pathway splices X-box binding protein-1 (XBP-1) mRNA into its spliced form XBP-1s, which then transcriptionally activates many downstream targets (i.e. Edem1 and $P58^{ipk}$) to restore ER homeostasis (Ron and Walter 2007). Our previous study showed that the inhibition of IRE-1α/XBP-1s pathway mitigated prolonged Cd treatment induced apoptosis in HK-2 cells (Ge et al. 2018). In addition, silver nanoparticles (15 nm in size) degraded the ER stress sensor ATF-6 protein, leading to the activation of the NLRP3 inflammasome and pyroptosis in human THP-1 monocytes (Simard et al. 2015).

Sirtuin-1 (SIRT1), a NAD^+-dependent class III lysine deacetylase, is the mammalian homologue of yeast silent information regulator 2 (Sir2) and can be activated in response to various cellular stresses (Haigis and Sinclair 2010; Xiao et al. 2018). Activation of SIRT1 deacetylates the acetyl group on the lysine residues of proteins and thus modulates their biological functions (Blander and Guarente 2004). Liver-specific overexpression of SIRT1 in low-density lipoprotein receptor deficient mice attenuated high-fat/high-sucrose diet induced hepatic steatosis and insulin resistance, which correlated with the inhibition of ER stress and XBP-1 splicing (Li et al. 2011). A more recent in vivo study in mice reported that SIRT1-dependent inhibition of ER stress was mediated by deacetylating heat shock factor

1, which resulted in upregulation of heat shock protein 40 (HSP40) and HSP70, and thus normalization of ER stress in the liver (Zheng et al. 2017). Yet, whether and how SIRT1 modulates Cd-induced ER stress in renal tubular epithelial cell are not well-understood.

This study aimed to investigate whether Cd could induce pyroptosis and how SIRT1 and ER stress regulate Cd-mediated pyroptosis in HK-2 cells in vitro and in vivo. We found that Cd treatment downregulated SIRT1 expression and induced the NLRP3 inflammasome activation, ER stress and pyroptosis and that activation of SIRT1 by genetic and pharmacological approaches normalized Cd-induced these effects through deacetylation and inhibition of XBP-1s. These results identify a novel mechanism mediating Cd-induced cytotoxicity in renal epithelial cells and may provide new therapeutic strategies for the treatment of Cd exposure related renal diseases.

Materials and methods

Chemicals and reagents

Cadmium chloride ($CdCl_2$) and 4-phenyl butyric acid (4-PBA) were purchased from Sigma-Aldrich (St. Louis, MO, USA). Fetal bovine serum (FBS) was obtained from GIBCO (Grand Island, NY, USA). RPMI 1640 medium was purchased from Corning (Manassas, VA, USA). Caspase-1 inhibitor (Z-YVAD-FMK) and SIRT1 activator (resveratrol) were purchased from Apex Bio (Boston, MA, USA) and IRE-1α inhibitor (STF-083010) was obtained from Selleckchem (Shanghai, China). Thapsigargin (Tg) was purchased from Abcam (Cambridge, UK). Rabbit monoclonal antibodies against human NLRP3, caspase-1, cleaved-caspase-1 (c-caspase-1), cleaved-IL-1β (c-IL-1β), ATF-6, PERK, IRE-1α, XBP-1s, SIRT1, nuclear factor (erythroid 2)-like 2 (NRF2), β-tubulin, β-actin and mouse monoclonal IL-1β antibody were purchased from Cell Signaling Technology (Danvers, MA, USA).

Cell culture and Cd treatment

Human renal proximal tubular epithelial (HK-2) cells were obtained from American Type Culture Collection (ATCC) and maintained in RPMI-1640 medium supplemented with 10% FBS and 1% penicillin/streptomycin in a humidified incubator with 5% CO_2 at 37 °C. For Cd treatment, HK-2 cells were seeded and allowed to attach for 24 h followed by Cd treatment (2–10 μM) in serum-free medium for 12 h or 48 h. The dosage was chosen based on previous work from our group and others (Ge et al. 2018; Olszowski et al. 2012) showing that Cd at micromolar concentrations (1–10 μM) could induce inflammation by activation of NF-κB pathway, upregulation of adhesion molecule expression and induction of proinflammatory cytokines and chemokines. Since we study inflammation-dependent pyroptosis, the 2–10 μM dose range was used in this study. For intervention experiments, HK-2 cells were pretreated with Z-YVAD-FMK (10 μM for 12 h), 4-PBA (5 mM for 24 h), resveratrol (10 μM for 12 h), or STF-083010 (30 μM for 12 h) followed by treating with 10 μM $CdCl_2$ for another 48 h. DMSO (final concentration < 0.1%) was included as vehicle control for all treatment conditions.

Cd treatment in mice

Six-week-old male C57BL/6 mice were purchased from Shanghai SLAC Laboratory Animal Co., Ltd (Shanghai, China) and housed under standard environmental conditions with room temperature of 22 °C, humidity of 40–70% and a 12:12 h light-dark cycle. All animal experiments were performed according to the Guidelines for Animal Welfare of Fudan University, the Guide for the Care and Use for Laboratory Animals published by the Ministry of Health of the People's Republic of China and the Guide of the Care and Use of Laboratory Animals (NIH Publication No. 85-23, revised 2011). 24 mice were randomly divided into four groups (6 mice per group) and exposed to 100, 200, or 400 mg/L $CdCl_2$ or DMSO vehicle control in drinking water for 12 weeks (Thijssen et al. 2007a). The concentrations of Cd we chose in this study were comparable with previously published Cd-induced nephrotoxicity in rodents (Brzoska et al. 2003; Liu et al. 2000; Thijssen et al. 2007a, b; Zeng et al. 2003). The dose of 100 mg/L $CdCl_2$ was considered to be relevant to the exposure levels of Cd in the environment (Thijssen et al. 2007b). The drinking water was changed every 2 days and the Cd doses were refreshed with each water change. The amount of water consumed by animals was monitored and no significant differences were found among different treatment groups. Animals were weighed weekly. After 12-week treatment, the mice were sacrificed under anesthesia and the kidneys were collected and immediately frozen in liquid nitrogen and stored at − 80 °C until analysis.

siRNA silencing of NLRP3 and XBP-1

After grown to 50% confluence, HK-2 cells were transfected with 100 pmol of siRNA targeting human NLRP3 (siNLRP3), or human XBP-1 (siXBP-1), or negative control siRNA (siNC) (Ribobio, Guangdong, China) using Lipo6000™ Transfection Reagent (Beyotime, Shanghai, China) according to the manufacturer's protocol. After 4 h of transfection, the medium was removed and replaced with fresh complete culture medium for 24 h before $CdCl_2$ treatment.

Overexpression of SIRT1, mutant SIRT1^{H363Y} and XBP-1s

Wide-type SIRT1 or mutated SIRT1 (SIRT1^{H363Y}) was overexpressed in HK-2 cells using cytomegalovirus (CMV) promoter driven plasmid containing human wide-type SIRT1 cDNA (pCDH-SIRT1) or human mutated SIRT1 cDNA lacking deacetylase activity (pCDH-SIRT1^{H363Y}), respectively (Shanghai Yuanmin Biotech, Shanghai, China). XBP-1s was overexpressed using CMV-promoter driven plasmid containing human XBP-1s cDNA (pCDH-XBP-1s) (Shanghai Yuanmin Biotech, Shanghai, China). HK-2 cells were transiently transfected with 5 μg of wide-type SIRT1, inactive SIRT1 mutant, XBP-1s, or empty control plasmid DNA (pCDH-Empty) in a 6-cm dish using Lipo6000™ according to the manufacturer's protocol. After 4 h of transfection, cells were cultured in fresh medium for 24 h followed by $CdCl_2$ treatment. The overexpression of SIRT1, SIRT1^{H363Y}, or XBP-1s was confirmed using quantitative RT-PCR or immunoblotting assays.

Enzyme-linked immunosorbent assay (ELISA)

At the end of $CdCl_2$ treatment (2–10 μM, 48 h), the culture supernatants of treated and untreated HK-2 cells were collected for the measurements of IL-6, IL-1β, IL-18, tumor necrosis factor α (TNF-α) and transforming growth factor β (TGF-β) levels using ELISA kits (R&D Systems, Minneapolis, MN, USA) according to the manufacturer's instructions.

Cytotoxicity assay

Cell death was evaluated by the release of lactate dehydrogenase (LDH) into the supernatants using a colorimetric LDH cytotoxicity kit (Dojindo; Shanghai, China). Briefly, after $CdCl_2$ treatment, the culture supernatants were harvested and incubated with LDH assay solutions for 30 min at 25 °C. The spectrophotometric absorbance of red formazan, which is directly proportional to LDH release was determined at 490 nm using the Synergt™ HT Microplate Reader (BioTek, Winooski, VT, USA). The percentage change of LDH release was calculated relative to untreated control cells.

Fluorescent staining of Hoechst 33342 and propidium iodide (PI)

Pore formation on cell membranes was evaluated using Hoechst 33342 and PI double-fluorescent staining. $CdCl_2$-treated and untreated control cells were washed with PBS and stained with Hoechst 33342 and PI (0.625 μg/mL) at 37 °C for 30 min in the dark. Cell images were recorded using a fluorescent microscope (Olympus, Tokyo, Japan) and analyzed using Image J software. The percentage of PI-positive cells were calculated by counting 1000 randomly selected nuclei for each treatment group.

Real-time polymerase chain reaction (RT-PCR)

Total RNA of HK-2 cells were extracted using Trizol reagent (Invitrogen, CA, USA) according to the manufacturer's protocol. The concentration and purity of isolated RNA were determined by NanoDrop 2000 spectrophotometer (Thermo Scientific, Waltham, MA, USA). Total RNA (2 μg) was reversely transcribed into cDNA using FastKing Reverse Transcriptase Kit (Tiangen, Beijing, China). cDNA samples and specific primers (Supplementary Table S1) were used to amplify the target genes using SuperReal PreMix Plus (SYBR Green) kits (Tiangen, Beijing, China) on an ABI 7300Plus fast Real-Time PCR system (Applied Biosystems, Foster City, CA, USA). GAPDH expression in each sample was included as internal control. Gene expression was quantitated using $2^{-\Delta\Delta Ct}$ method (Xiao et al. 2016).

Western blotting

Cellular total proteins were extracted using RIPA lysis buffer containing 1 mM PMSF (Beyotime, Shanghai, China) and the protein concentration was determined using BCA protein assay (Beyotime, Shanghai, China). 30 micrograms of total proteins were resolved on 12% SDS-PAGE gel and transferred to polyvinylidene difluoride membranes. Non-specific binding sites were blocked with 5% nonfat milk in TBST (100 mM Tris–HCl pH 7.4, 0.9% NaCl and 0.1% Tween 20) at room temperature for 4 h. The membranes were washed with TBST and incubated with specific primary antibodies against NLRP3 (1:1000), caspase-1 (1:1000), c-caspase-1 (1:1000), IL-1β (1:1000), c-IL-1β (1:1000), ATF6 (1:1000), PERK (1:1000), IRE-1α (1:1000), XBP-1s (1:1000), SIRT1 (1:1000), NRF2 (1:1000), β-tubulin (1:1000), β-actin (1:1000) overnight at 4 °C. The membranes were then incubated with anti-rabbit or anti-mouse HRP-conjugated IgG antibodies (1:2000) for 2 h at room temperature. The protein bands were visualized by ECL™ and Western Blotting Detection Reagents (Pierce Chemical, Dallas, TX, USA). The densitometry was evaluated using Image J software.

Isolation of nuclear proteins

Nuclear extracts were prepared using Nuclear and Cytoplasmic Protein Extraction Kit (Beyotime, Shanghai, China). Briefly, cells were scraped in cytosolic protein extraction reagent and centrifugated. The cell pellet was subsequently incubated in nuclear protein isolation buffer for 30 min on ice with frequent vortex. Nuclear extracts in the supernatant were collected by centrifugation and protein concentration was determined by BCA protein assay.

SIRT1 activity

SIRT1 enzymatic activity was assayed using a colorimetric kit (Genmed, China). Simply, 50 micrograms of cellular total proteins were incubated with synthesized substrates containing acetylated lysine residue [Ac-Arg-His-Lys-Lys (Ac)] at 30 °C for 45 min. The reaction was terminated by incubating with Stopping Buffer and peptidase for additional 30 min at 30 °C. SIRT1 activity was then determined by the measurement of absorbance at 405 nm using the Synergt™ HT Microplate Reader (BioTek, Winooski, VT, USA). Protein concentration of each sample was used to normalize SIRT1 activity.

Co-immunoprecipitation

The interaction between SIRT1 and XBP-1s, as well as the levels of XBP-1s acetylation were evaluate using Universal Magnetic Co-IP Kit (Active Motif, CA, USA). Total cellular proteins were incubated with SIRT1 antibody or α-acetyllysine (Cell Signaling Technology, Danvers, MA, USA) for 4 h at 4 °C. Subsequently, the protein mixtures were incubated with Protein G Magnetic Beads for 1 h at 4 °C. The pellets were washed four times on magnetic stand and resuspended in loading buffer. The immunoprecipitant pellets were analyzed using anti-SIRT1 and anti-XBP-1s antibodies by immunoblotting assay.

Statistical analyses

All data were presented as mean ± SEM. One-way analysis of variance (ANOVA) followed by multiple range least significant difference (LSD) test was used to assess difference among different groups. p values < 0.05 were considered statistically significant. All statistical analyses were performed with SPSS 20.0 for Windows (IBM, Armonk, NY, USA).

Results

Cd triggers pyroptosis in human renal HK-2 cells in vitro and mouse kidneys in vivo

Pyroptosis is a novel type of programmed cell death and has been shown in Cd-induced cell death in HUVEC (Bergsbaken et al. 2009; Chen et al. 2016). Yet, it remains unclear whether pyroptosis is involved in Cd-induced cytotoxicity in human and mouse renal epithelial cells. Therefore, we studied the effects of Cd on pyroptosis in vitro and in vivo. We first determined the mRNA and protein expression of pyroptosis-related genes in HK-2 cells treated with different concentrations of $CdCl_2$ (2–10 μM) for 12 h or 48 h. We observed that Cd treatment upregulated NLRP3 protein levels by two-to-threefold and increased the levels of both cleaved-caspase-1 (c-caspase-1) and cleaved-IL-1β (c-IL-1β) by roughly twofold at 48 h compared to control cells; while the levels of pro-caspase-1 and pro-IL-1β were not significantly affected (Fig. 1a). Results from RT-PCR showed that Cd also significantly and dose-dependently upregulated NLRP3, caspase-1, GSDMD and ASC mRNA expression at 48 h; albeit these changes were much less obvious at 12 h of Cd treatment (Fig. 1b, c). Importantly, the protein levels of NLRP3, c-caspase-1 and c-IL-1β were also enhanced by three-to-fivefold in mouse kidneys treated with different concentrations Cd for 12 weeks in vivo (Fig. 1d). Moreover, the Cd-induced upregulation of these pyroptosis-related genes was correlated with increased LDH release (Fig. 2a), which is a marker of cell death caused by compromised cell membrane. Consistently, Cd treatment also tremendously increased the percentage of PI positive cell population to 20–60% compared to 4% in untreated control cells (Fig. 2b). This effect was absent after 12 h of Cd treatment (Suppl. Fig. 1). Thus, these results suggest a correlation between the activation of pyroptosis-related genes and Cd-induced cell death in vitro and in vivo.

To confirm pyroptosis is the mechanism mediating Cd-induced cytotoxicity, we inhibited caspase-1 activity in HK-2 cells since pyroptosis depends on caspase-1 activation (Bergsbaken and Cookson 2007; Chen et al. 2016; Fink et al. 2008). HK-2 cells were pretreated with a caspase-1 inhibitor, Z-YVAD-FMK (YVAD; 10 μM) followed by 10 μM of $CdCl_2$ treatment for 48 h. We found that YVAD pretreatment significantly inhibited basal levels of c-caspase-1 protein, confirming the efficacy of YVAD as a caspase-1 inhibitor in HK-2 cells (Fig. 2c). Importantly, we also found that pretreatment of YVAD partially but significantly abrogated Cd-induced the upregulation of c-caspase-1 and c-IL-β protein levels, which correlated with significant reductions of Cd-induced LDH release and increase in the percentage of PI-positive cells (Fig. 2c–e). Therefore, these results from in vitro and in vivo studies suggest that $CdCl_2$ induces caspase-1-dependent pyroptosis in human renal HK-2 cells and mouse kidneys.

Cd treatment induces pro-inflammatory microenvironment in HK-2 cells

Since the release of pro-inflammatory cytokines is a hallmark of pyroptosis (Bergsbaken et al. 2009), we next determined the expression and secretion of cytokines in $CdCl_2$ treated HK-2 cells. As shown in Fig. 2a, the mRNA levels of IL-6, IL-18 and IL-1β increased by two-to-threefold after $CdCl_2$ treatment (6–10 μM); while TNF-α mRNA expression was slightly upregulated and TGF-β expression was no noticeable difference (Fig. 3a). Furthermore, we also

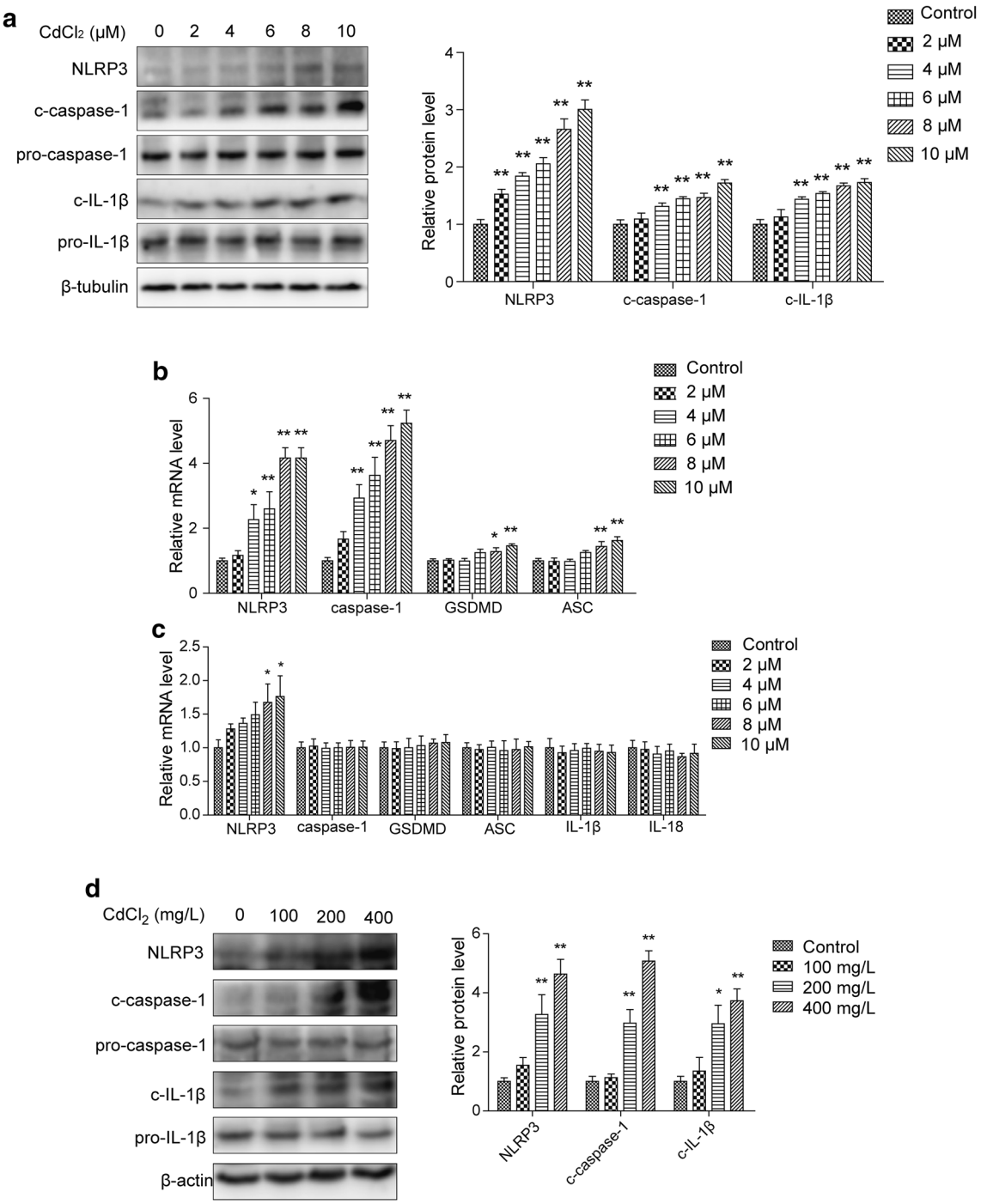

Fig. 1 Cd upregulates pyroptosis-related gene expression in vitro and in vivo. HK-2 cells were treated with different doses of Cd (2–10 μM) for 48 h (**a, b**) or 12 h (**c**). **a** Cd treatment activated NLRP3 inflammasome. Representative immunoblotting images (left panel) and quantitative results (right panel) showed the protein levels of NLRP3, cleaved caspase-1 (c-caspase-1) and cleaved IL-1β (c-IL-1β) in control and Cd-treated cells. β-tubulin was used as internal control. **b** RT-PCR results showed that the expression levels of NLRP3, caspase-1, GSDMD and ASC mRNA were significantly upregulated in Cd-challenged HK-2 cells compared to control cells. **c** RT-PCR results showed that Cd treatment (12 h) upregulated NLRP3 mRNA expression but not caspase-1, GSDMD, ASC, IL-1β and IL-18 mRNA. Fold change in all panels was calculated relative to untreated control cells. $*p<0.05$ and $**p<0.01$ compared to untreated group; $n=3$. **d** The expression levels of the NLRP3 inflammasome related proteins were upregulated in the kidneys of Cd-treated mice. Adult male C57BL/6 mice were fed with different doses of Cd (100–400 mg/L) or DMSO vehicle control in drinking water for 12 weeks. Left panel: representative immunoblotting images; β-actin was included as loading control. Right panel: quantitative analysis. Fold change was calculated relative to vehicle treated mice. $*p<0.05$ and $**p<0.01$ compared to vehicle control group; $n=6$

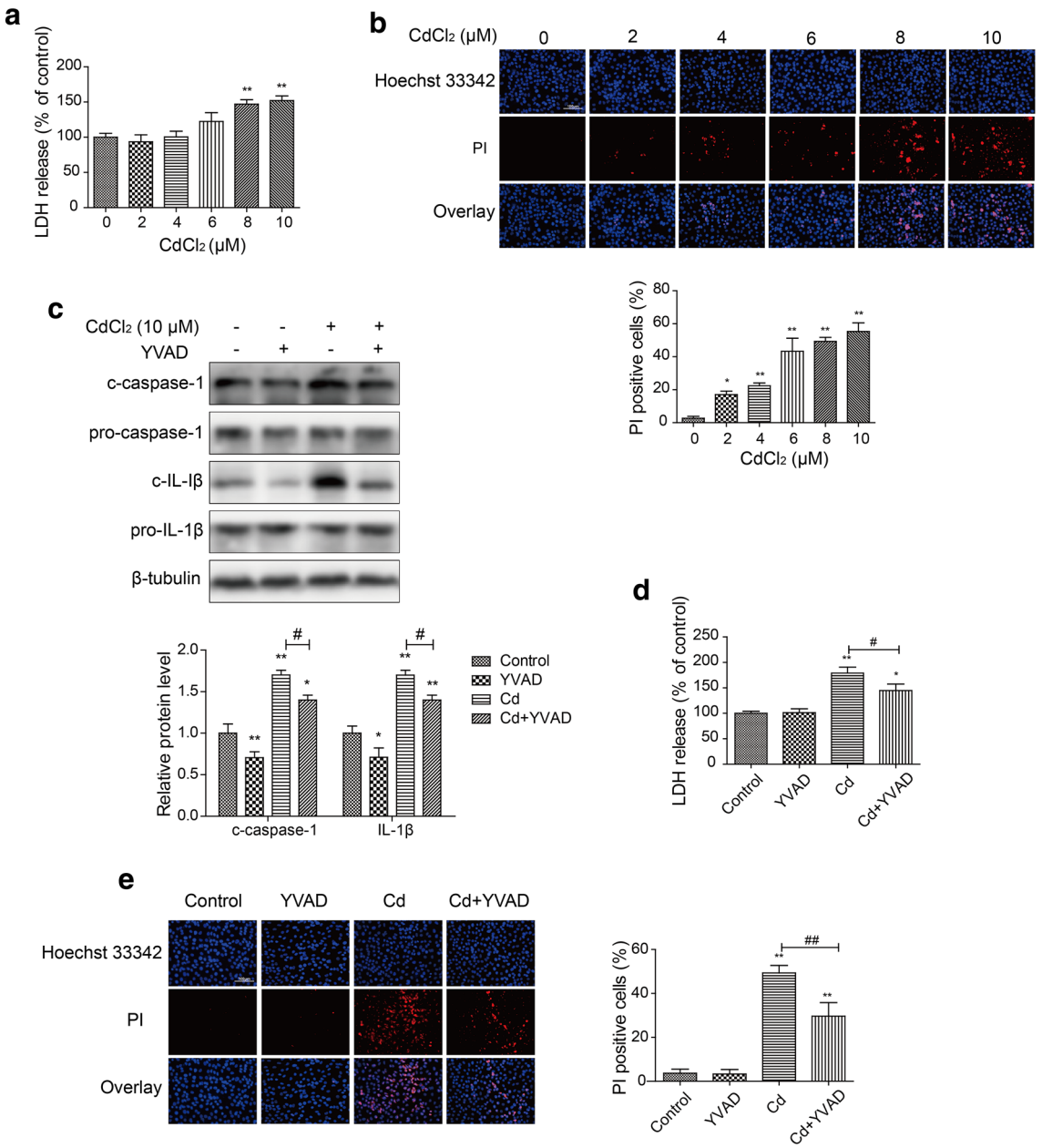

Fig. 2 Cd induces caspase-1-dependent inflammatory pyroptosis in HK-2 cells. Cells were treated with different doses of Cd (2–10 μM) for 48 h. **a** The release of LDH was elevated in Cd-treated HK-2 cells. LDH in culture medium was determined using a colorimetric LDH cytotoxicity kit. **b** The percentage of PI positive cells increased in HK-2 cells post 48 h of Cd treatment. Left panel: representative fluorescent imaged of PI (dead cells) and Hoechst 33342 (nucleus) staining in untreated and Cd-treated cells. Magnification: ×200; scale bar = 100 μm. Right panel: the corresponding quantification (%) of PI positive cells. **c** Inhibition of caspase-1 with a pharmacological inhibitor YVAD abrogated Cd-induced increases in c-caspase-1 and c-IL-1β protein levels. HK-2 cells were pretreated with 10 μM Z-YVAD-FMK (YVAD) for 12 h and then treated with $CdCl_2$ (10 μM for 48 h). Representative immunoblotting images (left panel) and quantitation results (right panels) were shown. Inhibition of caspase-1 with YVAD aborted Cd-induced increases in LDH release (**d**) and PI-positive cell population (**e**). HK-2 cells were treated as described above. Cells were labeled with PI Hoechst 33342 for dead cells and nucleus, respectively. Image magnification: ×200; scale bar = 100 μm. Fold change in all panels was calculated relative to untreated control cells. $^{*}p < 0.05$ and $^{**}p < 0.01$ compared to untreated group; $^{\#}p < 0.05$ and $^{\#\#}p < 0.01$ compared to Cd treated cells; $n = 3$

measured the protein levels of these cytokines in the culture media using ELISA assays. Consistent with the mRNA expression results, the secreted levels of IL-6, IL-18, IL-1β and TNF-α were significantly higher in Cd-treated cells than untreated controls; whereas the extracellular levels of TGF-β remained unaffected (Fig. 3b). These data indicated that

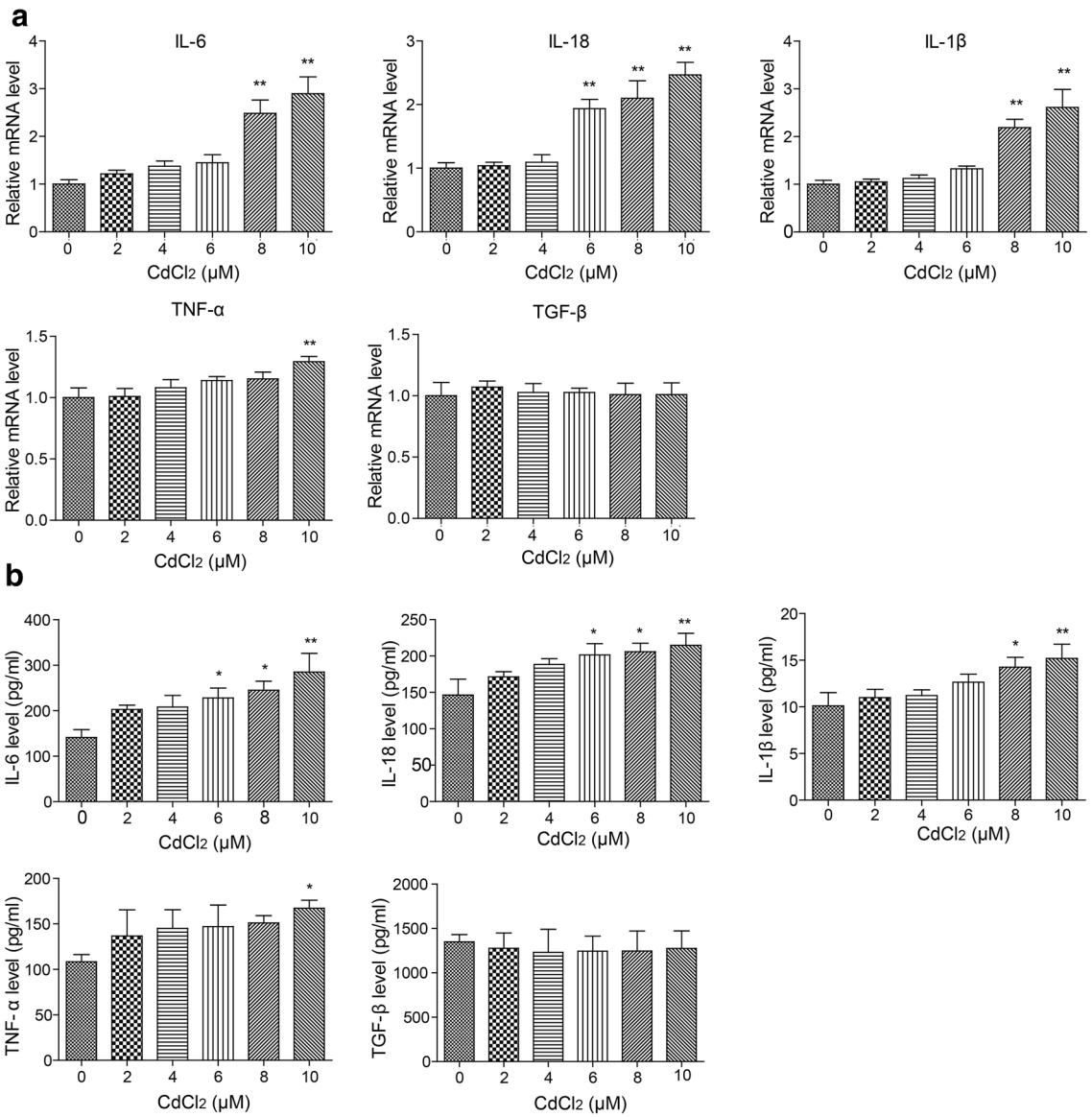

Fig. 3 Cd increases the expression and secretion of inflammatory cytokines in HK-2 cells. HK-2 cells were treated with different concentrations of $CdCl_2$ (2–10 μM) for 48 h. The mRNA expression (**a**) and secretion (**b**) of IL-6, IL-18, IL-1β, TNF-α and TGF-β were measured using RT-PCR and ELISA assays, respectively. Fold change was calculated relative to untreated control cells. $^{*}p<0.05$, $^{**}p<0.01$ compared to untreated controls; $n=3$

$CdCl_2$ (6–10 μM) induces pro-inflammatory phenotype in HK-2 cells, which further supports Cd-induced pyroptosis.

The NLRP3 inflammasome activation mediates Cd-induced pyroptosis in HK-2 cells

It is known that increased levels of c-caspase-1 and mature IL-1β as well as mature IL-18 are hallmarks of the NLRP3 inflammasome activation (Takahashi 2014). Our results in Figs. 1 and 3 showed that Cd treatment enhanced NLRP3 expression and increased the levels of c-caspase-1, IL-18 and IL-1β, suggesting that the NLRP3 inflammasome is activated by Cd in HK-2 cells. Since the NLRP3 inflammasome and other inflammasomes (e.g. NLRC4) have been implicated in pyroptosis (Cerqueira et al. 2015), we examined whether the NLRP3 inflammasome is the key mediator of Cd-induced pyroptosis by silencing NLRP3 expression with siRNA. We first confirmed the efficiency of NLRP3 knockdown and found that transfection with siNLRP3 set no. 2 decreased the NLRP3 protein levels by 50% in HK-2 cells (Suppl. Fig. 2). Therefore, this set of siNLRP3 was used throughout this study. Interestingly, NLRP3 silencing significantly mitigated Cd-induced increases in mRNA levels of NLRP3 and caspase-1, the mRNA levels

of pyroptosis-related genes (GSDMD and ASC) and the mRNA levels of pro-inflammatory genes (IL-1β and IL-18) (Fig. 4a). Likewise, the upregulated levels of NLRP3, c-caspase-1 and c-IL-1β proteins in Cd-treated cells were also significantly attenuated by knockdown of NLRP3 (Fig. 4b). Furthermore, silencing of NLRP3 also abrogated Cd-induced increases in the release of LDH and the percentage of PI positive cells (Fig. 4c, d). Thus, these findings indicate that NLRP3 activation is the primary mechanism mediating Cd-induced pyroptotic cell death in HK-2 cells.

ER stress mediates Cd-induced NLRP3 activation and pyroposis in HK-2 cells

We next investigated the mechanisms underlying Cd-induced the NLRP3 inflammasome activation. Recently, our results showed that chronic treatment with $CdCl_2$ (1 μM for 12 days) activated ER stress in HK-2 cells (Ge et al. 2018). Lebeaupin et al. (2015) reported that lipopolysaccharide (LPS)-induced ER stress activated the NLRP3 inflammasome in mouse liver in vivo and in cultured primary mouse hepatocytes. Thus, we hypothesized that Cd-induced activation of the NLRP3 inflammasome is mediated by ER stress in HK-2 cells. We first detected the expression of ER stress marker genes in HK-2 cells treated with Cd for 12 h or 48 h. In line with our previous results of chronic Cd treatment (Ge et al. 2018), we found that Cd treatment upregulated the protein levels of ATF6, PERK and IRE-1α as well as its downstream target XBP-1s by approximately two-to-threefold at 48 h (Fig. 5a), which correlated with upregulated mRNA expression of the members of the ATF6 branch [Grp78 (two-to-fourfold), Grp94 (two-to-eightfold), Pida4 (1.5-fold) and Calreticulin (two-to-threefold)], the PERK branch [ATF4 (three-to-fivefold), ATF3 (two-to-fourfold), Gadd34 (two-to-fourfold) and Chop (four-to-sixfold)] and the IRE-1α branch [IRE-1α (1.5- to 2.5-fold), XBP-1s (twofold), Edem1 (two-to-threefold) and $P58^{ipk}$ (two-to-eightfold)] (Suppl. Fig. 3a–c). By contrast, treatment with Cd for 12 h also induced a dose-dependent upregulation of the mRNA levels of the PERK branch markers and the IRE-1α branch markers, but barely affected the expression of the ATF6 branch related markers (Suppl. Fig. 3d–f). These results thus suggest that all three branches of ER stress are activated in Cd-treated HK-2 cells. Together with results in Figs. 1, 2, 3 and 4, our findings also indicate that ER stress correlates with Cd-induced activation of the NLRP3 inflammasome and pyroptosis in HK-2 cells.

To test this correlation, we treated HK-2 cells with thapsigargin (Tg), a widely-used ER stress stimulant (Kato et al. 2012). As expected, Tg treatment activated all three ER branches in HK-2 cells (Suppl. Fig. 4a). Surprisingly, Tg treatment also upregulated the mRNA expression of the NLRP3 inflammasome- and pyroptosis-related genes including NLRP3, caspase-1, GSDMD, ASC, IL-1β and IL-18 by four- to-sevenfold (Suppl. Fig. 4b), supporting that ER stress modulates pyroptosis in HK-2 cells. To further confirm ER stress mediates Cd-induced activation of the NLRP3 inflammasome and pyroptosis, we inhibited ER stress by pretreating HK-2 cells with 4-PBA, a classic ER stress inhibitor (Li et al. 2018). 4-PBA is a low molecular weight chemical chaperone and can inhibit ER stress through stabilization of protein conformation and degradation of misfolded proteins (Burrows et al. 2000; Yam et al. 2007). We found that 4-PBA significantly inhibited the basal levels of ATF6, PERK, IRE-1α and XBP-1s protein (Fig. 5b, Suppl. Fig. 3g), confirming the efficacy of 4-PBA as an ER stress inhibitor in HK-2 cells, which is consistent with previous findings in the same cell line (Fan et al. 2015). Furthermore, we also found that 4-PBA pretreatment partially but significantly mitigated Cd-induced upregulation of proteins in all three ER stress branches (Fig. 5b, Suppl. Fig. 3g). Notably, 4-PBA pretreatment significantly attenuated the elevated protein levels of NLRP3, c-caspase-1 and c-IL-1β in Cd-treated cells (Fig. 5c, Suppl. Fig. 3h), which was accompanied with a marked normalization of the mRNA expression of NLRP3 inflammasome- and pyroptosis-related genes (NLRP3, caspase-1, GSDMD, ASC, mature IL-1β and mature IL-18) (Fig. 5d). These results suggest that inhibition of ER stress can block Cd-induced activation of the NLRP3 inflammasome and perhaps pyroptosis in HK-2 cells. Indeed, the inhibition of pyroptosis by 4-PBA was supported by results showed in Fig. 5e, f. Pretreating with 4-PBA significantly mitigated Cd-induced increases in LDH release and the percentage of PI-positive cells (Fig. 5e, f). Overall, our finding demonstrate that ER stress mediates Cd-induced activation of the NLRP3 inflammasome-dependent pyroptosis in HK-2 cells.

The IRE-1α/XBP-1s branch is required for Cd-induced activation of NLRP3 inflammasome and pyroptosis in HK-2 cells

We next investigated whether the IRE-1α/XBP-1s branch is the primary pathway regulating Cd-induced activation of the NLRP3 inflammasome and pyroptosis in HK-2 cells since we recently reported that activation of the IRE-1α/XBP-1s branch of ER stress promoted apoptosis induced by chronic Cd treatment (Ge et al. 2018). We used a small molecule inhibitor STF-083010, which specifically inhibits the endonuclease activity of IRE-1α leading to inhibition of the IRE-1α/XBP-1s branch (Papandreou et al. 2011). HK-2 cells were pretreated with STF-083010 (30 μM, 12 h) followed by 48 h of Cd treatment. Results showed that pretreatment with STF-080310 significantly mitigated the increased levels of NLRP3, c-caspase-1 and c-IL-1β proteins in Cd-treated cells (Fig. 6a), which was associated with inhibition of Cd-induced upregulation of the NLRP3 inflammasome-related genes (NLRP3, mature IL-1β and mature IL-18 mRNA)

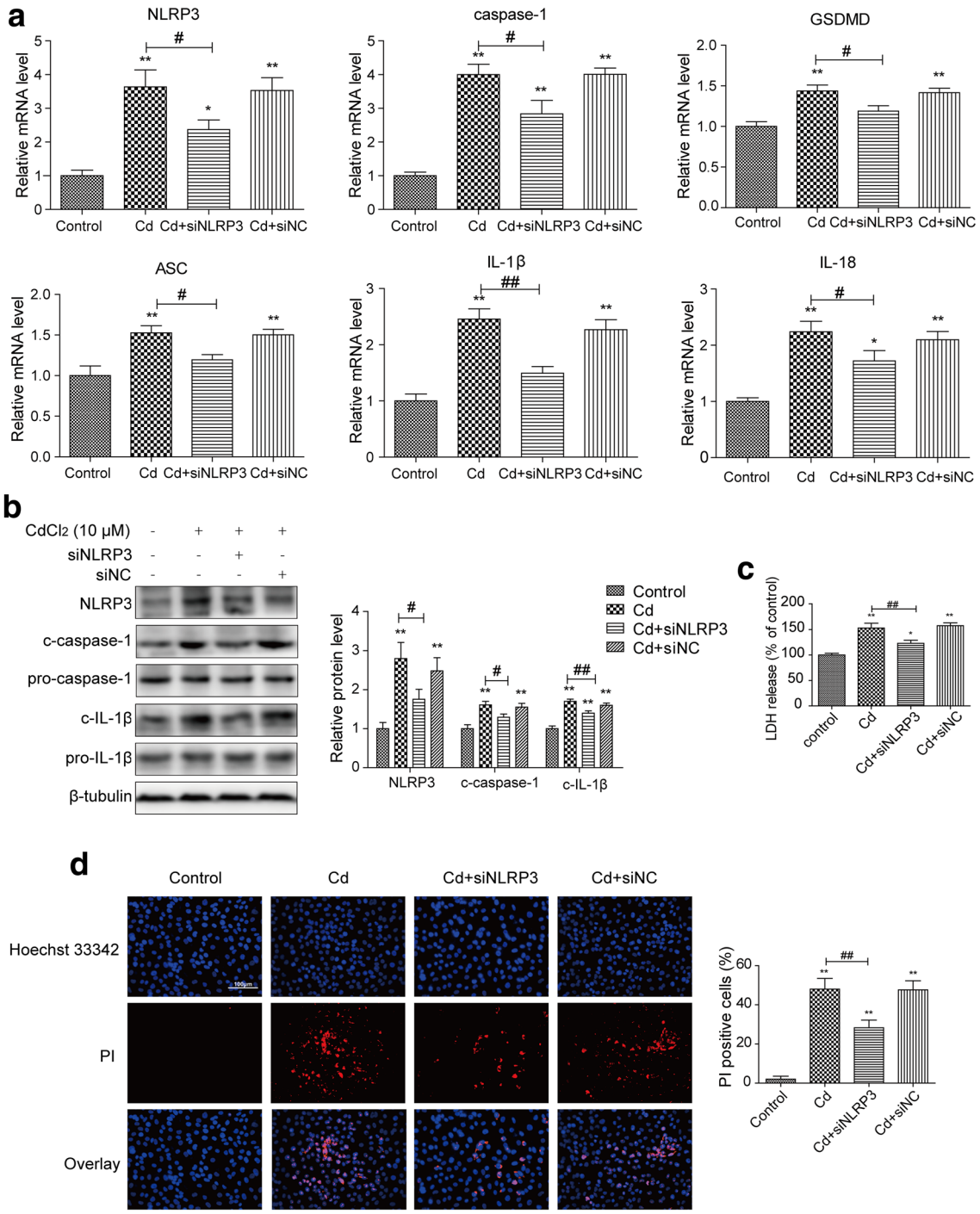

Fig. 4 NLRP3 silencing inhibits Cd-induced NLRP3 activation and pyroptosis in HK-2 cells. HK-2 cells were transfected with negative control siRNA (siNC) or NLRP3 siRNA (siNLRP3) followed by 48 h treatment of 10 μM $CdCl_2$. **a** NLRP3 knockdown mitigated Cd-induced upregulation of the NLRP3 inflammasome genes (NLRP3, caspase-1, IL-1β and IL-18 mRNA) and pyroptosis related genes (GSDMD and ASC mRNA). Fold change was calculated relative to control cells. **b** Immunoblotting images (left panel) and quantitative results (right panel) showed that knockdown of NLRP3 significantly ablated Cd-induced increases in NLRP3, c-caspase-1 and c-IL-1β protein levels in HK-2 cells. Fold change was calculated relative to control cells. Silencing NLRP3 in HK-2 cells significantly suppressed the increases in LDH release (**c**) and the percentage of PI-positive cells (**d**) induced by Cd treatment. **c** The relative LDH release in siNC or siNLRP3 transfected cells in presence or absence of Cd treatment. **d** Representative images of PI positive cells (left panel) and the calculated percentage of PI positive cells (right panel) in siNC or siNLRP3 transfected cells with or without Cd treatment. Magnification: ×200; scale bar = 100 μm. $^{*}p < 0.05$ and $^{**}p < 0.01$ compared to untreated group; $^{\#}p < 0.05$ and $^{\#\#}p < 0.01$ compared to Cd treatment group; $n = 3$

(Fig. 6b), suggesting that inhibition of the IRE-1α/XBP-1s branch attenuates the NLRP3 inflammasome activation. Of note, STF-083010 pretreatment also abrogated Cd-induced augment in nuclear NRF2 protein levels and upregulation of metallothionein 1 (MT1) and MT2 mRNA expression in HK-2 cells (Suppl. Fig. 5).

To investigate whether IRE-1α/XBP-1s regulates pyroptosis, we measured pyroptosis-related gene expression and cell death in cells with or without this inhibitor. Interestingly, we observed that Cd-induced upregulations of caspase-1, GSDMD and ASC mRNA were significantly abrogated by STF-080310 pretreatment (Fig. 6b). Importantly, we also found that the inhibition of IRE-1α/XBP-1s branch by STF-083010 markedly attenuated Cd-induced elevations in LDH release and the percentage of PI positive cells (Fig. 6c, d). To further consolidate these results, we silenced XBP-1 with siRNA in HK-2 cells followed by Cd treatment. As expected, XBP-1 knockdown abrogated Cd-induced increase in XBP-1s protein levels (Suppl. Fig. 6a,b). Notably, XBP-1 silencing also substantially aborted Cd-induced upregulation of NLRP3, caspase-1, GSDMD and ASC mRNA expression, which correlated with a reduction in LDH release (Fig. 6e, f). Together, these results suggest that activation of the IRE-1α/XBP-1s branch is required for Cd-induced the NLRP3 inflammasome-dependent pyroptosis in HK-2 cells.

SIRT1 inhibits Cd-induced ER stress via selectively deacetylating XBP-1s

SIRT1 is known as a stress-response protein deacetylase (Brunet et al. 2004). Prola et al. (2017) demonstrated that SIRT1 activation protected cardiomyocytes against ER-stress induced cell death in vivo and in vitro. We thus studied the potential roles of SIRT1 in regulating Cd-induced ER stress. We first measured SIRT1 expression in HK-2 cells post 48 h of Cd treatment (2–10 μM). Consistent with previous report in HepG2 cells (Guo et al. 2014), we found that Cd suppressed SIRT1 protein levels and its activity by 20–40% in HK-2 cells (Fig. 7a, b). Interestingly, the suppression of SIRT1 was accompanied with the activation of ER stress (Fig. 5a, Suppl. Fig. 3a–f), suggesting a negative correlation between SIRT1 expression and ER stress in Cd-treated HK-2 cells.

To further explore the roles of SIRT1 in Cd-induced ER stress, we pretreated HK-2 cells with resveratrol, a pharmacological activator of SIRT1 (Guo et al. 2015). Resveratrol pretreatment increased the basal SIRT1 protein levels by 1.5-fold (Fig. 7c, Suppl. Fig. 7a). More importantly, pretreating with resveratrol significantly inhibited Cd-induced downregulation of SIRT1 protein and upregulation of XBP-1s protein; albeit it did not affect the increased levels of ATF6, PERK and IRE-1α proteins (Fig. 7c, Supp. Fig. 7a). To further validate these results, we overexpressed SIRT1 in HK-2 cells followed by Cd treatment. An approximately threefold increase in SIRT1 protein was detected in SIRT1-containing plasmid transfected cells compared to empty-vector transfected cells (Suppl. Fig. 7b). In line with results in Fig. 7c, SIRT1 overexpression significantly abrogated Cd-induced SIRT1 downregulation, but did not impact Cd-induced upregulations of the ATF6 protein, the ATF6 branch genes (Grp78, Grp94, Pdia4 and Calreticulin mRNA expression), the PERK protein and the PERK branch genes (ATF3, ATF4, Chop and Gadd34 mRNA expression) (Fig. 7d, Suppl. Fig. 7c–f). Strikingly, ectopic overexpression of SIRT1 significantly mitigated Cd-induced increases in XBP-1s mRNA and protein expression, as well as the mRNA levels of its downstream targets Edem1 and $P58^{ipk}$ (Fig. 7d, Suppl. Fig. 7e); however, it failed to attenuate Cd-induced IRE-1α upregulation (Fig. 7d, Suppl. Fig. 7e, f). These results suggest that SIRT1 inhibits Cd-induced ER stress by selectively inhibiting the IRE-1α/XBP-1s branch in HK-2 cells.

SIRT1 regulates protein function through deacetylation on lysine residues. Since SIRT1 did not affect IRE-1α upregulation but indeed abrogated the upregulation of its downstream target XBP-1s protein in Cd-treated cells, we hypothesized that SIRT1 directly and physically interact with XBP-1s. To investigate this hypothesis, proteins bound to SIRT1 were immunoprecipitated and the presence of XBP-1s was detected in the pulldowns. As expected, the XBP-1s protein was detected in the SIRT1 immunoprecipitants in untreated control cells (Fig. 7e), suggesting SIRT1 physically interacts with XBP-1s in HK-2 cells. Interestingly, this physical interaction was significantly attenuated by Cd treatment (Fig. 7e), which correlated with decreases in SIRT1 protein levels and activity (Fig. 7a, b). These results reveal that Cd treatment inhibits the binding of SIRT1 with XBP-1s through suppression of SIRT1 protein in HK-2 cells.

We next investigated whether SIRT1 regulates the acetylation of XBP-1s protein. Total proteins with acetylated lysine residues were pulled down from HK-2 cells lysates. The acetylated levels of XBP-1s were significantly higher in Cd treated cells than untreated control cells (Fig. 7f), suggesting Cd-induced SIRT1 suppression leads to accumulation of acetylated XBP-1s protein. Intriguingly, overexpression of SIRT1 completely ablated the acetylated XBP-1s protein levels in Cd-treated cells (Fig. 7f). To further validate that XBP-1s deacetylation is mediated by SIRT1, a dominant negative SIRT1 plasmid (pCDH-$SIRT1^{H363Y}$) was used to overexpress a mutant protein lacking deacetylase activity (Vaziri et al. 2001) (Suppl. Fig. 7b and h). We

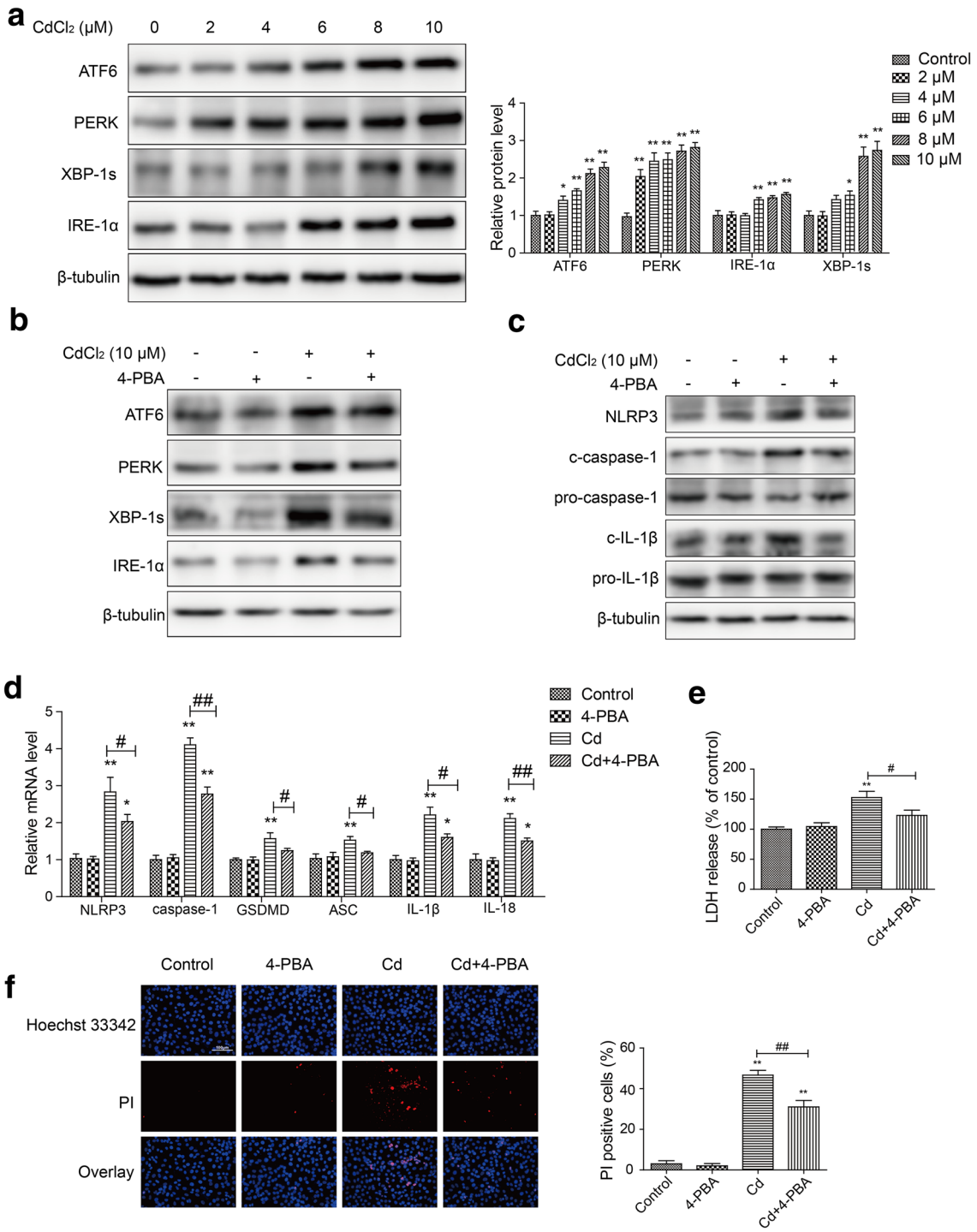

found that the overexpression of this mutated SIRT1 failed to abrogate Cd-induced decrease in SIRT1 activity and accumulation of XBP-1s acetylation (Fig. 7g, h; Suppl. Fig. 7g, h). Together, these results indicate that SIRT1 selectively inhibits Cd-induced activation of the IRE-1α/XBP-1s branch of ER stress through directly deacetylating XBP-1s protein in HK-2 cells.

SIRT1 overexpression blocks Cd-induced the NLRP3 inflammasome activation and pyroptosis via inhibition of the IRE-1α/XBP-1s pathway in HK-2 cells

We next examined the effects of SIRT1 overexpression on Cd-induced activation of the NLRP3 inflammasome and pyroptosis in HK-2 cells. Our results showed that the

◂**Fig. 5** ER stress mediates Cd-induced NLRP3 activation and pyroptosis in HK-2 cells. **a** Cd activated three ER stress pathways in HK-2 cells. The protein levels of ATF6, PERK, IRE-1α and XBP-1s were determined by immunoblotting in cells treated with vehicle control or Cd as indicated doses for 48 h. Representative immunoblotting images (left panel) and the quantitative results (right panel) were shown. **b** Inhibition of ER stress by 4-PBA abrogated Cd-induced upregulation of ER stress proteins. HK-2 cells were pretreated with ER stress inhibitor 4-PBA (5 mM) for 24 h and then treated with Cd (10 μM) for 48 h. Representative immunoblotting images showed the levels of ER stress response proteins. β-tubulin was included as loading control. **c** 4-PBA pretreatment inhibited Cd-induced upregulation of the NLRP3 inflammasome related proteins. Cd treatments were performed as described in panel b. The level of the NLRP3 inflammasome related proteins were determined. β-tubulin was included as loading control. **d** 4-PBA pretreatment abrogated Cd-induced upregulations of the NLRP3 inflammasome-related gene expression. Cells were treated as described in **b**. mRNA expression was determined by RT-PCR. Fold change was calculated relative to untreated control cells. **e** 4-PBA pretreatment inhibited Cd-induced LDH release in HK-2 cells. The release of LDH in cell culture medium was calculated relative to controls. **f** 4-PBA pretreatment inhibited Cd-induced cytotoxicity. Cd treatments were performed as described in **b**. The dead cells were determined by PI and Hoechst 33342 co-staining (left panel) using fluorescent microscopy. The quantitation (right panel) was performed using Image J software. Magnification: ×200; scale bar = 100 μm. For all panels, $^{*}p < 0.05$ and $^{**}p < 0.01$ when compared to untreated control cells; $^{\#}p < 0.05$ and $^{\#\#}p < 0.01$ compared to Cd-treated cells; $n = 3$

overexpression of SIRT1 completely aborted the upregulated protein levels of NLRP3, c-caspase-1 and c-IL-1β in Cd-exposed cells (Fig. 8a), which correlated with a marked inhibition of Cd-induced increases in NLRP3, mature IL-1β and mature IL-18 mRNA expression (Fig. 8b). Moreover, we also found that overexpressing SIRT1 significantly abrogated Cd-induced elevations in the mRNA expression of pyroptosis-related genes caspase-1, GSDMD and ASC (Fig. 8b), which were accompanied with a significant suppression of Cd-induced increases in LDH release and PI positive cells (Fig. 8c, d), suggesting SIRT1 overexpression protects HK-2 cells from Cd-induced activation of the NLRP3 inflammasome and pyroptosis.

We next determined if the protective effects of SIRT1 overexpression are mediated by targeting the IRE-1α/XBP-1s pathway. HK-2 cells were simultaneously co-transfected with human SIRT1 and XBP-1s containing plasmids. The overexpression of XBP-1s was confirmed by immunoblotting assay showing an approximately fourfold increase in XBP-1s protein levels in cells transfected with XBP-1s-containing plasmid compared to empty-vector transfected cells (Suppl. Fig. 8a). In line with results described above (Figs. 7d, 8a–c), SIRT1 overexpression alone significantly abrogated Cd-induced upregulation of XBP-1s, NLRP3, c-caspase-1 and c-IL-1β protein levels and increase in LDH release. Intriguingly, SIRT1-mediated these protective effects were markedly reversed in cells with co-overexpression of both SIRT1 and XBP-1s (Fig. 8e, f, Suppl. Fig. 8b). Therefore, these results together with results in Fig. 7 clearly indicate that SIRT1 protects HK-2 cells against Cd-induced pyroptosis through deacetylating XBP-1s protein and thereby inhibiting the IRE-1α/XBP-1s branch of ER stress.

Discussion

Cd-induced nephrotoxicity is primarily through damages of proximal tubular cells. The underlying mechanisms of Cd-induced renal nephrotoxicity require better understanding. In this study, we used in vivo mouse model and in vitro cell culture model to investigate the potential mechanisms of Cd-induced nephrotoxicity. Our results reveal for the first time that pyroptosis, a caspase-1- and NLRP3-inflammasome-dependent programmed cell death mechanism mediates Cd-induced toxicity in human and mouse renal cells. We also demonstrate that the enhancement of SIRT1 activity by pharmacological and genetic means mitigates Cd-induced activation of the NLRP3 inflammasome and pyroptosis through deacetylating XBP-1s protein and thus inhibiting the IRE-1α/XBP-1s pathway (Fig. 9).

Mounting evidence from our group and others demonstrated that Cd treatment could induce apoptosis or/and autophagy in human and rodent renal tubular epithelial cells (Ge et al. 2018; Gu et al. 2018; Liu et al. 2016). Unlike apoptosis and autophagy, pyroptosis, a recently identified programmed cell death mechanism, is less understood in Cd-induced cytotoxicity. Pyroptosis is characterized by its dependence on the NLRP3 inflammasome and caspase-1 protein (Bergsbaken et al. 2009). Our results showed that Cd treatment significantly upregulated the expression of the NLRP3 inflammasome- and pyroptosis-related genes (e.g. NLRP3, ASC, GSDMD, cleaved caspase-1, cleaved IL-1β and cleaved IL-18) in HK-2 cells and mouse kidneys (Fig. 1), which correlated with increased transcription and secretion of pro-inflammatory cytokines and decreased cell survival in HK-2 cells (Figs. 1, 2, 3). Importantly, inhibition of caspase-1 activity with an inhibitor Z-YVAD-FMK or knockdown of NLRP3 with siRNA substantially mitigated Cd-induced activation of the NLRP3 inflammasome (e.g. upregulated expression of NLRP3, c-caspase 1 and c-IL-1β proteins) and increase in cell death (Figs. 2, 4). These results indicate that Cd induces the NLRP3 inflammasome- and caspase-1-dependent pyroptosis in HK-2 cells. Liu et al. (2017) reported that ionizing radiation activated the NLRP3 inflammasome and increased protein levels of cleaved caspase-1 leading to pyroptosis in cultured mouse bone-marrow deprived macrophages (BMDM), all of which were significantly suppressed in BMDM isolated from NLRP3 knockout mice. To date,

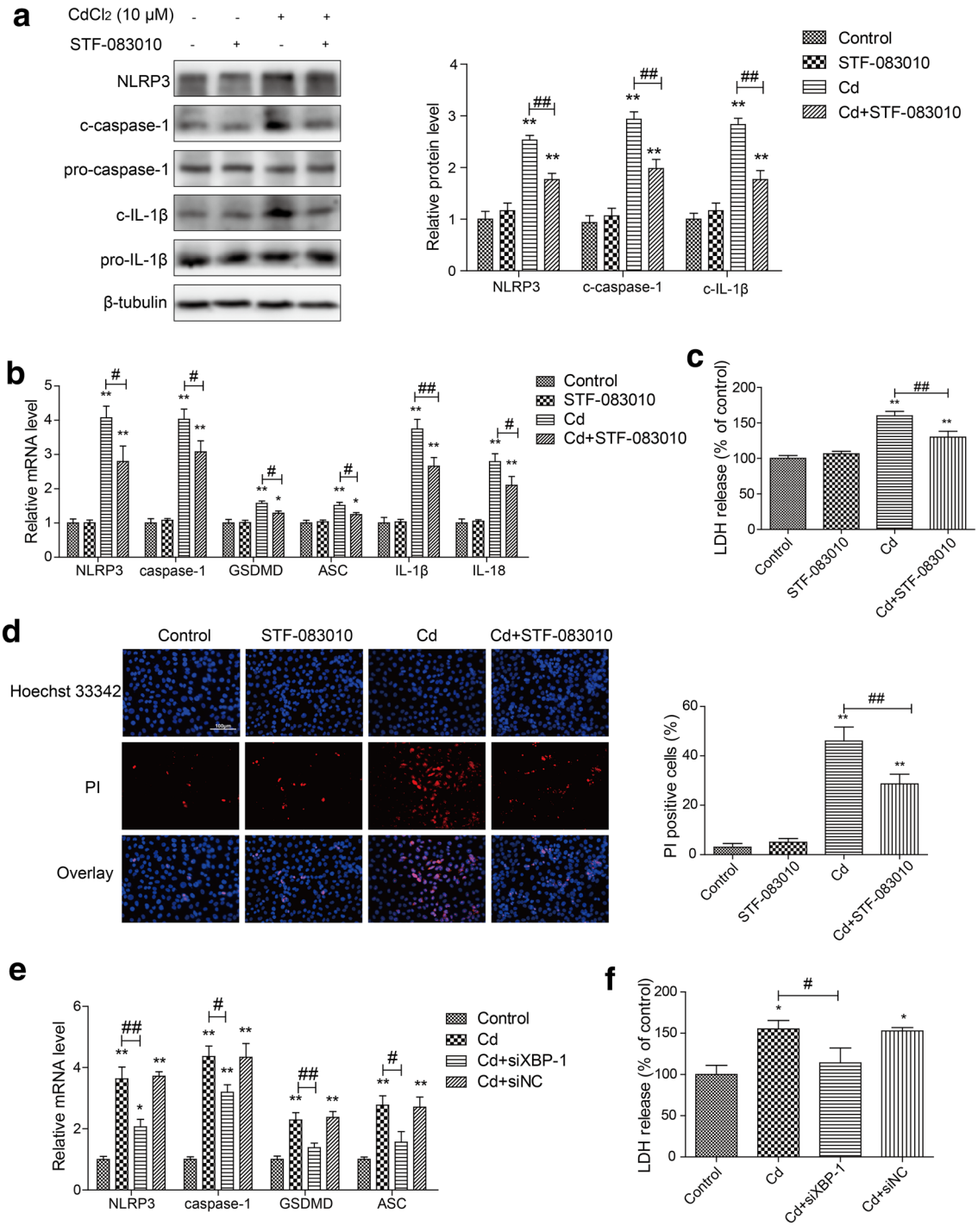

few studies shed light on the role of pyroptosis in Cd-induced cell death. In HUVEC, treatment with Cd activated the NLRP3 inflammasome and elevated cleaved caspase-1 protein levels resulting in pyroptosis, which was inhibited by knockdown of NLRP3 (Chen et al. 2016). Similar findings were observed in cultured human hepatocytes treated with Cd-containing quantum dots (Lu et al. 2016). Moreover, these Cd-containing quantum dots could induce hepatic inflammation and dysfunctions in NLRP3 wide-type mice; by contrast, NLRP3 knockout mice were resistant to these toxic effects (Lu et al. 2016). Overall, the NLRP3 inflammasome- and caspase-1-dependent pyroptosis emerges as a novel mechanism mediating Cd-induced cytotoxicity.

◂**Fig. 6** The IRE-1α/XBP-1s branch is required for Cd-induced NLRP3 inflammasome activation and pyroptosis in HK-2 cells. The IRE-1α/XBP-1s branch was inhibited using a specific inhibitor STF-080310. HK-2 cells were pretreated with 30 μM STF-080310 for 12 h, followed by another 48 h of 10 μM Cd treatment. **a** STF-083010 significantly reversed Cd-induced increased expression of the NLRP3 inflammasome-related proteins. Representative immunoblotting images (left panel) and the quantitative results (right panel) were shown. β-tubulin was included as loading control. Fold change was calculated relative to control cells. **b** STF-083010 pretreatment abrogated Cd-induced upregulation of the NLRP3 inflammasome-related genes. mRNA expression was determined by RT-PCR. Fold change was calculated relative to untreated controls. **c** Cd-induced increases in LDH release (**c**) and PI positive cell population (**d**) were significantly alleviated by pretreating with STF-083010. Image magnification: ×200; scale bar = 100 μm. **e** Silencing XBP-1 mitigated Cd-induced upregulation of mRNA expression in the NLRP3 inflammasome. HK-2 cells were transfected with control siRNA (siNC) or XBP-1siRNA (siXBP-1) followed by Cd treatment (10 μM for 48 h). mRNA expression was determined by RT-PCR. Fold change was calculated relative to untreated and siNC transfected cells. **f** XBP-1 knockdown abrogated Cd-induced LDH release in HK-2 cells. Cells were treated as described in **e**. For all panels, $^{*}p < 0.05$ and $^{**}p < 0.01$ when compared to untreated control group; $^{\#}p < 0.05$ and $^{\#\#}p < 0.01$ compared to Cd treatment group; $n = 3$

Increasing in vitro and in vivo evidence demonstrated that Cd treatment activated ER stress, which contributed to Cd-induced apoptosis or/and autophagy in HK-2 cells (Ge et al. 2018), porcine renal proximal tubular cell line LLC-PK1 (Yokouchi et al. 2007) and HEK cells as well as mouse kidneys (Luo et al. 2016). Moreover, two independent groups demonstrated that the activation of ER stress (the IRE-1α and the PERK pathways) promoted the NLRP3 inflammasome activation, caspase-1 cleavage and IL-1β secretion in human and rodent pancreatic β cells (Lerner et al. 2012; Oslowski et al. 2012). We, therefore, examined whether ER stress can regulate Cd-induced the NLRP3 inflammasome activation and pyroptosis in HK-2 cells. Consistent with our previous results (Ge et al. 2018), the three ER stress branches (the IRE-1α branch, the ATF-6 branch and the PERK branch) were activated by Cd treatment (Fig. 5 and Suppl. Fig. 3). Intriguingly, pretreatment with an ER stress inhibitor 4-PBA significantly mitigated Cd-induced ER stress, upregulation of the NLRP3 inflammasome-related genes and pyroptosis (Fig. 5, Suppl. Fig. 3). To identify the crucial ER stress branch in regulating Cd-induced pyroptosis, we focused on the well-studied IRE-1α pathway. IRE-1α can splice 26 nucleotides from its target XBP-1 mRNA into the spliced mRNA XBP-1s via its RNase activity (Kriss et al. 2012). The splicing leads to the formation of a 371-amino acid functional transcriptional factor XBP-1s, which transcriptionally activates the expression a series of ER stress genes including Edem1 and P58^{ipk} to restore ER homeostasis (Lee et al. 2003). We blocked the IRE-1α/XBP-1s branch, using siRNA-mediated XBP-1 silencing and a small molecule inhibitor STF-083010, which specifically inhibits the RNase activity of IRE-1α (Papandreou et al. 2011). Like 4-PBA, inhibition of the IRE-1α/XBP-1s pathway by both means also significantly alleviated Cd-induced activation of the NLRP3 inflammasome and pyroptosis in HK-2 cells (Fig. 6, Suppl. Fig. 6). Although no evidence reported the roles of ER stress in modulating Cd-induced the NLRP3 inflammasome activation and pyroptosis, our results were supported by other in vivo and in vitro models. For example, in an ischemia–reperfusion (IR)-induced kidney injury rat model, Yang et al. (2014) found that IR significantly enhanced pyroptosis-related protein levels (cleaved caspase-1 and IL-1β), which correlated with upregulation of ER stress marker proteins Grp78 and Chop in renal tissue. These findings were recapitulated in rat renal tubular epithelial NRK-52E cells challenged with hypoxia-reoxygenation (HR) (Yang et al. 2014). Silencing Chop with siRNA abrogated HR-induced increases in cleaved caspase-1 and IL-1β protein levels and pyroptosis in NRK-52E cells (Yang et al. 2014). Moreover, pretreatment with STF-083010 significantly attenuated ER stress inducer thapsigargin-induced XBP-1s splicing, which correlated with an inhibition of IL-1β secretion in human THP-1 cells (Lerner et al. 2012). Taken together, our results demonstrate that, for the first time, ER stress likely the IRE-1α/XBP-1s branch promotes the NLRP3 inflammasome-dependent pyroptosis in Cd-stimulated HK-2 cells.

Activation of the UPR in a short period of time can restore ER homeostasis and promote cell survival, whereas prolonged activation of the UPR results in cell death (Ron and Walter 2007; Schroder 2008; Xu et al. 2005). Our results showed that Cd treatment at 12 h activated ER stress but had no impacts on cell death (Fig. 1, Suppl. Figs. 1 and 3). However, when cells were treated with Cd for 48 h, activation of ER stress was accompanied with pyroptosis and inhibition of ER stress, particularly the IRE-1α/XBP-1s pathway protected cells from pyroptosis (Figs. 5, 6). These findings support that ER stress activation is an adaptive survival mechanism at earlier time (12 h) of Cd treatment, while it promotes cell death as Cd treatment extends (48 h) in HK-2 cells. Of note, it is possible that the inhibition of ER stress may also impact other cell survival mechanisms. To explore this possibility, we focused on two Cd-related survival mechanisms: the NRF2 pathway and the metal stress response pathway. Upon activation, transcription factor NRF2 translocates into the nucleus, where it transcriptionally activates a battery of antioxidant genes to counteract oxidative stress and damages (Ma 2013; Wu et al. 2012). Induction of MT proteins (MT1 and MT2) is also a protective mechanism in response to acute Cd exposure since MTs are small metal-binding

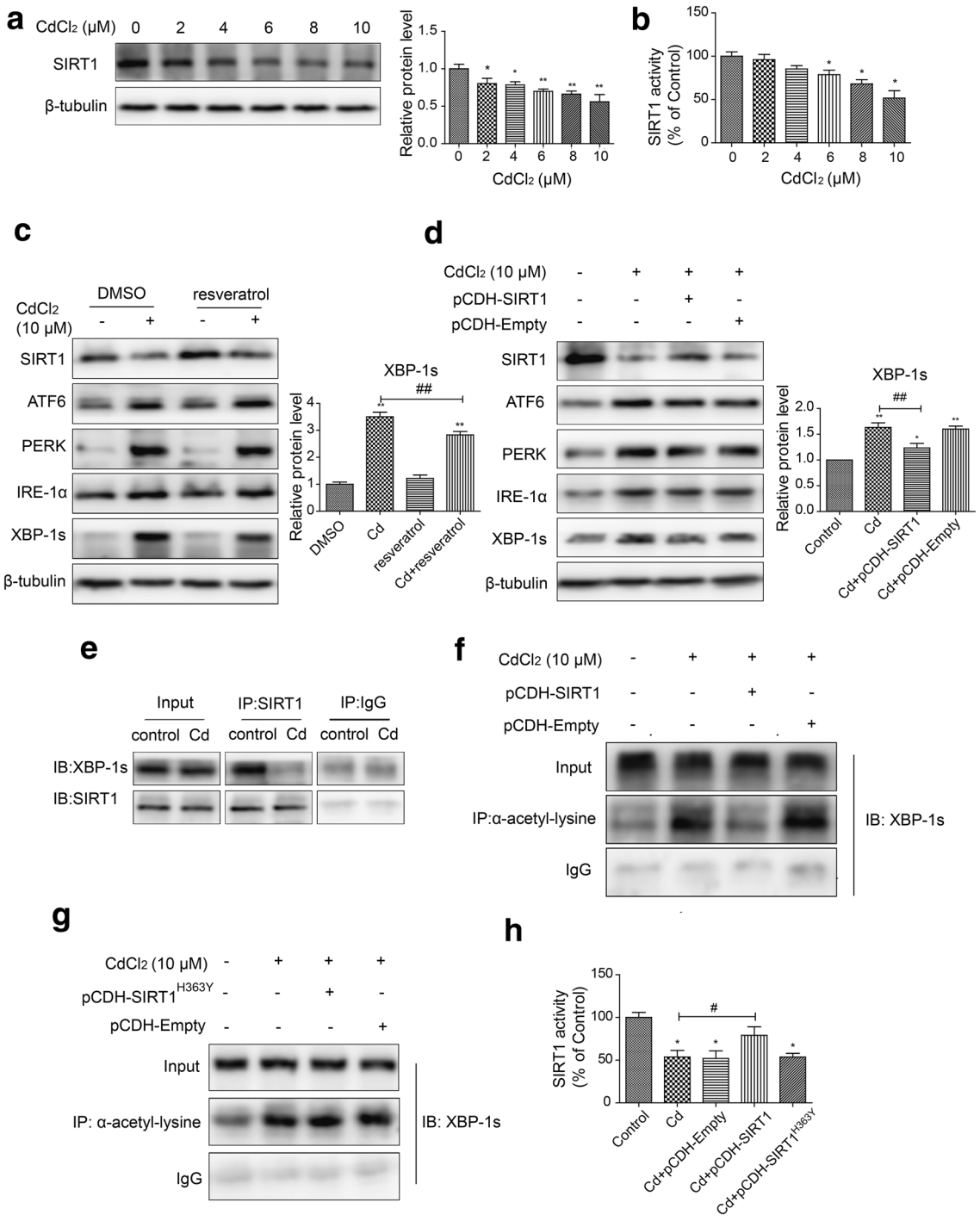

proteins and can directly conjugate Cd molecule (Klaassen et al. 2009; Sabolic et al. 2010). In addition, MT proteins are also thiol-containing proteins and can neutralize Cd-induced oxidative stress (Klaassen et al. 2009; Sabolic et al. 2010). We found in this work that Cd treatment (10 μM, 48 h) increased nuclear NRF2 protein levels and stimulated MT1 and MT2 mRNA expression in HK-2 cells (Suppl. Fig. 5). Recently, results from our group and others revealed that Cd treatment elevated cellular hydrogen peroxide levels in HK-2 cells (Ge et al. 2018; Wilmes et al. 2011), which correlated with activation of the NRF2 signaling evidence by the increase in nuclear translocation of NRF2 protein

◂**Fig. 7** SIRT1 selectively inhibits Cd-induced activation of the IRE-1α/XBP-1s branch via deacetylating XBP-1s. **a** The protein level and activity **b** of SIRT1 were suppressed in HK-2 cells after treatment with indicated doses of Cd for 48 h. **c** SIRT1 activity activator resveratrol selectively suppressed Cd-induced upregulation of XBP-1s protein. HK-2 cells were pretreated with resveratrol (10 μM for 12 h) and then treated with 10 μM Cd for 48 h. Representative immunoblotting images of marker proteins of the three ER stress branches (left panel) and quantitation of XBP-1s protein level (right panel) were shown. Fold change was calculated related to untreated controls. **d** Overexpression of SIRT1 selectively inhibited the increase of XBP-1s protein levels in Cd-treated cells. HK-2 cells were transfected with empty (pCDH-Empty) or human SIRT1 cDNA containing plasmid (pCDH-SIRT1). After transfection, cells were treated with vehicle control or 10 μM $CdCl_2$ for 48 h. Representative immunoblotting images of marker proteins of the three ER stress branches (left panel) and quantitative results of XBP-1s protein (right panel) were shown. Fold change was calculated related to untreated controls. **e** Cd treatment decreased the physical binding of endogenous SIRT1 and XBP-1s proteins in HK-2 cells. Cells were treated with 10 μM $CdCl_2$ for 48 h. The proteins bound to SIRT1 were first immunoprecipitated from total cellular proteins using specific human SIRT1 antibody. Immunoblotting analysis of XBP-1s was used to test the binding of SIRT1 with XBP-1s. IgG was used as negative controls. Immunoblotting analysis of SIRT1 was included as loading controls. **f** SIRT1 overexpression reversed Cd-induced increase of XBP-1s acetylation level. Cells were treated as described in **d**. Total cellular proteins were first immunoprecipitated using antibody against α-acetyl-lysine followed by immunoblotting analysis of the acetylation of XBP-1s using specific antibody against human XBP-1s. IgG was included as negative controls and Input was used as loading controls. Overexpression of dominant negative SIRT1 ($SIRT1^{H363Y}$) failed to inhibit Cd-induced SIRT1 acetylation (**g**) and restore Cd-induced suppression of SIRT1 activity (**h**). Cells were transfected with Empty, wide-type SIRT1, or mutant $SIRT1^{H363Y}$ plasmid followed by Cd treatment as indicated dose for 48 h. For **a**–**d** and **h**, $^{*}p<0.05$ and $^{**}p<0.01$ when compared to untreated control group; $^{\#}p<0.05$ and $^{\#\#}p<0.01$ compared to Cd treatment group; $n=3$

and the upregulation of its down-stream target genes [e.g. heme-oxygenase 1 (HO-1)] (Wilmes et al. 2011). Furthermore, Cd treatment also enhanced HO-1, MT1 and MT2 protein expression in primary human proximal tubular epithelial cells and HK-2 cells (Boonprasert et al. 2016). Therefore, these lines of evidence together with our findings clearly indicate that both the NRF2 signaling and the MT-mediated stress response pathway are active in response to Cd in human renal cells. Surprisingly, we also found that Cd-induced activation of these two protective pathways was attenuated by inhibition of the IRE-1α/XBP-1s pathway since the inhibitor STF-083010 pretreatment abrogated Cd-induced upregulation of NRF2 and MTs expression (Suppl. Fig. 5). One possible explanation for this phenomenon could be that under the blockade of the IRE-1α/XBP-1s pathway, Cd-treated cells exhibited less pyroptotic cell death, which thereby relieves the activation of these two protective mechanisms. However, the exact mechanisms and the potential biological consequences require future investigation.

To understand how Cd activates the IRE-1α/XBP-1s pathway, we focused on protein deacetylase SIRT1 since it is highly expressed in proximal tubule cells and podocytes in the kidney (Morigi et al. 2018). Importantly, SIRT1 could bind to and deacetylate PERK protein; and inhibition of SIRT1 activity using pharmacological inhibitor or siRNA activated the PERK/eIF2α branch of ER stress resulting in apoptosis in cultured rat primary chondrocytes (Kang et al. 2018). Our results showed that Cd treatment significantly suppressed SIRT1 protein levels and enzymatic activity (Fig. 7), which correlated with activation of ER stress (Fig. 5). Notably, enhancement of SIRT1 activity using pharmacological agonist resveratrol or genetic SIRT1 overexpression selectively abrogated the induction of XBP-1s protein in Cd-treated HK-2 cells; while the induction of IRE-1α, ATF6 and PERK proteins was not significantly affected (Fig. 7, Suppl. Fig. 7). Mechanistically, Cd treatment decreased physical binding of SIRT1 with XBP-1s leading to decrease in XBP-1s deacetylation, and thus increase in its transcriptional activity, which were counteracted by overexpression of wide-type SIRT1 but not $SIRT1^{H363Y}$ mutant lacking deacetylase activity (Fig. 7, Suppl. Fig. 7), suggesting that XBP-1s deacetylation requires SIRT1 activity. Indeed, using purified acetylated XBP1s and SIRT1 proteins, Wang et al. (2011a) demonstrated that XBP-1s was a direct target of SIRT1 and its transcriptional activity was suppressed by SIRT1-mediated deacetylation. These authors also found that inhibition of SIRT1 activity by a specific inhibitor EX-527 or shRNA-mediated knockdown increased XBP-1s acetylation and that overexpression of SIRT1 deacetylated XBP-1s leading to the suppression of its transcriptional activity in HEK293 cells (Wang et al. 2011a). Overexpression of SIRT1 inhibited high-fat/high-sucrose diet induced ER stress and XBP-1 splicing in the liver of low-density lipoprotein receptor deficient mice (Li et al. 2011). Furthermore, resveratrol increased the binding of SIRT1 with XBP-1s leading to selective inhibition of XBP-1s transcriptional activity in human melanoma cells (Wang et al. 2011b). Together, these lines of evidence indicate that XBP-1s is target of SIRT1 deacetylase and that Cd inhibits SIRT1 activity leading to the accumulation of acetylated XBP-1s levels, and thus activation of the IRE-1α/XBP-1s pathway.

Results in Figs. 6 and 7 clearly demonstrated that the IRE-1α/XBP-1s pathway mediates the NLRP3 inflammasome activation and pyroptosis and that Cd-induced SIRT1 repression led to the activation of the IRE-1α/

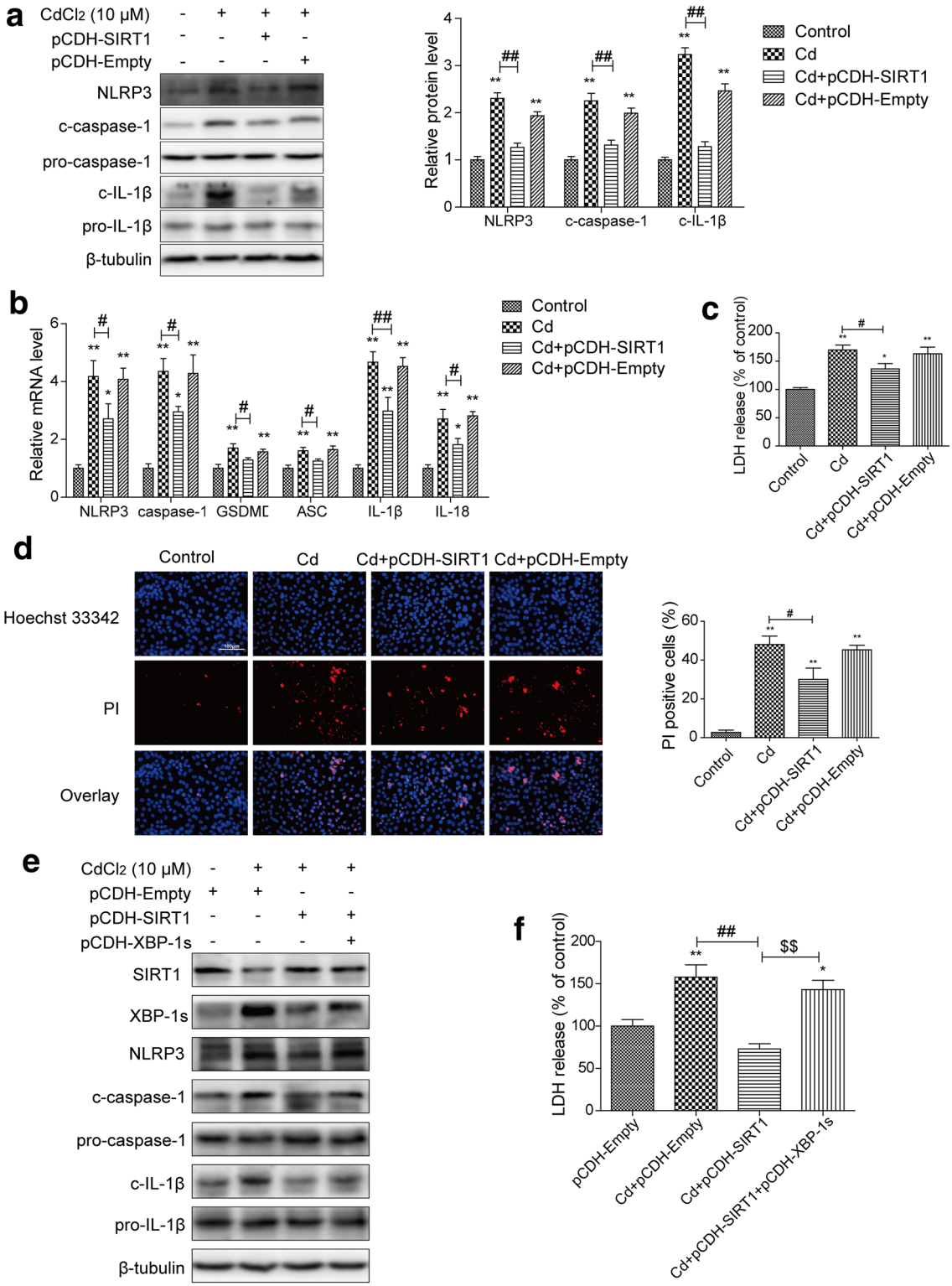
a
CdCl2 (10 μM) - + + +
pCDH-SIRT1 - - + -
pCDH-Empty - - - +
NLRP3
c-caspase-1
pro-caspase-1
c-IL-1β
pro-IL-1β
β-tubulin
Relative protein level
Control
Cd
Cd+pCDH-SIRT1
Cd+pCDH-Empty
NLRP3
c-caspase-1
c-IL-1β
b
Relative mRNA level
NLRP3
caspase-1
GSDMD
ASC
IL-1β
IL-18
c
LDH release (% of control)
d
Control
Cd
Cd+pCDH-SIRT1
Cd+pCDH-Empty
Hoechst 33342
PI
Overlay
PI positive cells (%)
e
CdCl2 (10 μM) - + + +
pCDH-Empty + + - -
pCDH-SIRT1 - - + +
pCDH-XBP-1s - - - +
SIRT1
XBP-1s
NLRP3
c-caspase-1
pro-caspase-1
c-IL-1β
pro-IL-1β
β-tubulin
f
LDH release (% of control)
pCDH-Empty
Cd+pCDH-Empty
Cd+pCDH-SIRT1
Cd+pCDH-SIRT1+pCDH-XBP-1s

◂**Fig. 8** SIRT1 overexpression mitigates Cd-induced NLRP3 inflammasome activation and pyroptosis in HK-2 cells. Empty or SIRT1 plasmid transfected cells were treated with 10 μM $CdCl_2$ for 48 h. **a** Overexpression of SIRT1 abrogated the activation of NLRP3 inflammasome induced by Cd. Representative immunoblotting images (left panel) and quantitative results (right panel) were shown. β-tubulin was included as loading control. **b** RT-PCR results showed that overexpressing SIRT1 aborted the upregulated mRNA expression of the NLRP3 inflammasome-related genes in Cd-treated cells. Fold change was calculated relative to untreated control cells. SIRT1 overexpression normalized Cd-induced increases in the LDH release (**c**) and the percentage of PI-positive cells (**d**). Image magnification: ×200; scale bar = 100 μm. Overexpression of XBP-1s opposes SIRT1-mediated inhibitions of the NLRP3 inflammasome activation (**e**) and LDH release (**f**) in Cd-treated cells. HK-2 cells were transfected with human SIRT1 cDNA containing plasmid (pCDH-SIRT1) or co-transfected with both pCDH-SIRT1 and human XBP-1s cDNA containing plasmid (pCDH-XBP-1s) followed by treatment with 10 μM $CdCl_2$ for 48 h. Representative immunoblotting images of SIRT1, XBP-1s and the NLRP3 inflammasome-related proteins (**e**) and the release of LDH (**f**) were shown. β-tubulin was included as loading control. For all panels, $^{*}p < 0.05$ and $^{**}p < 0.01$ when compared to untreated control group; $^{\#}p < 0.05$ and $^{\#\#}p < 0.01$ compared to Cd treatment group; $^{\$}p < 0.05$ and $^{\$\$}p < 0.01$ compared to Cd + pCDH-SIRT1 group; $n = 3$

XBP-1s pathway. Therefore, we explored whether SIRT1 could modulate the NLRP3 inflammasome and pyroptosis in Cd-treated cells. We found that the overexpression of SIRT1 significantly abrogated Cd-induced upregulation of the NLRP3 inflammasome- and pyroptosis-related genes, which correlated with marked reduction in pyroptotic cell death in Cd-treated cells (Fig. 8). Notably, these protective effects were opposed by ectopic co-overexpression of SIRT1 and XBP-1s (Fig. 8, Suppl. Fig. 8), suggesting SIRT1 activity protects against Cd-induced the NLRP3 inflammasome activation and pyroptosis in HK-2 cells through deacetylating XBP-1s protein and thus inhibiting its transcriptional activity. Chen et al. (2018a) found that hypoxia in combination with TNF-α repressed SIRT1 expression, which correlated with activation of the NLRP3 inflammasome and pyroptosis in H9c2 cardiomyoblasts and that these effects were mitigated when SIRT1 expression was restored by pretreatment with a glucagon-like peptide-1 analog liraglutide. Similarly, decreases in hepatic SIRT1 protein and activity were associated with activation of the NLRP3 inflammasome (upregulation of NLRP3 and caspase-1 protein and increases in proinflammatory cytokines IL-1, IL-6 and TNF-α levels) in the liver of mice fed with high-fat diet (Yang and Lim 2014). Supplementation of SIRT1 activator resveratrol normalized SIRT1 inhibition and protected against high-fat diet induced the NLPR3 inflammasome activation in the liver (Yang and Lim 2014). Moreover, resveratrol also inhibited the upregulation of NLRP3 and IL-1β expression in ionizing radiation-challenged mesenchymal stem cells or in a sepsis-associated encephalopathy mice model (Fu et al. 2013; Sui et al. 2016). The anti-inflammatory activity of resveratrol was dependent upon SIRT1 activity since inhibition of SIRT1 with chemical inhibitor nicotinamide or SIRT1 shRNA abolished these effects (Fu et al. 2013; Sui et al. 2016). In addition, Zhang et al. (2017) found that SIRT1 upregulation mediated the protective effects of dioscin on cisplatin-induced nephrotoxicity through deacetylation of NF-κB protein and activation of the NRF2 pathway leading to suppression of inflammation and oxidative stress in HK-2 cells. Overall, these findings reveal that SIRT1 activity can inhibit the NLRP3 inflammasome activation and potentially pyroptosis induced by various exogenous stimuli including Cd.

In conclusion, we discover that pyroptosis is a previously unrecognized inflammatory cell death mechanism mediating Cd-induced cytotoxicity and that SIRT1 protects against Cd-induced pyroptosis through deacetylation of XBP-1s protein leading to inhibition of the IRE-1α/XBP-1s pathway and the NLRP3 inflammasome in human tubular epithelial HK-2 cells. These findings may offer better understanding and novel therapeutic strategies for Cd-related chronic kidney diseases.

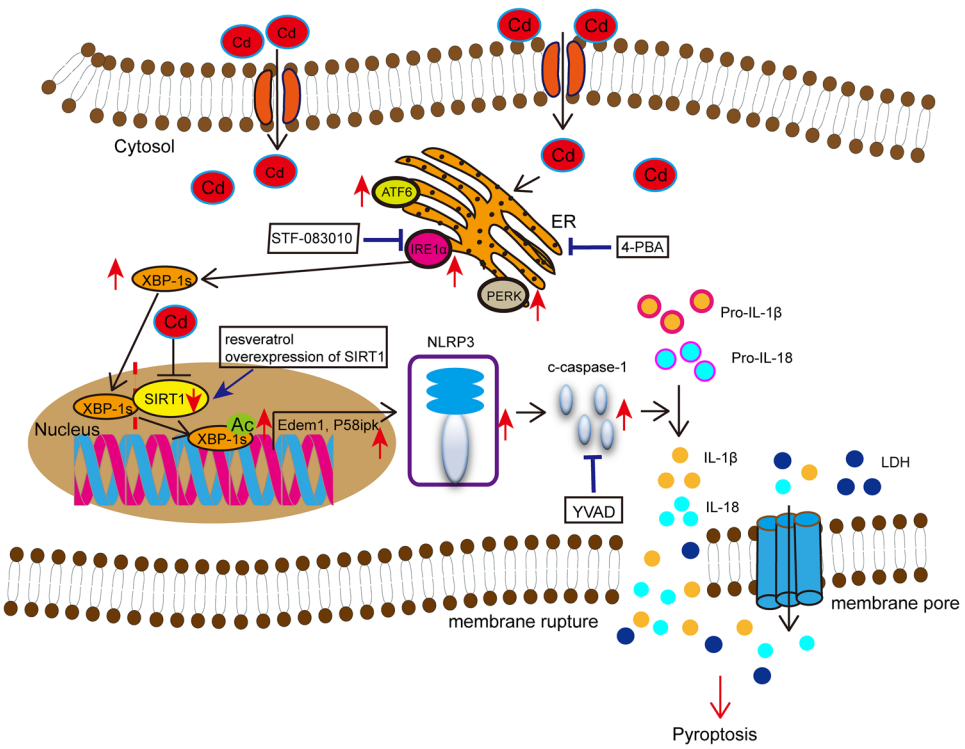

Fig. 9 Proposed mechanisms of Cd-induced pyroptosis in HK-2 cells. Cd treatment activated the three branches of ER stress and downregulated SIRT1 expression and activity. Cd-induced SIRT1 suppression led to accumulation of acetylated XBP-1s protein, and thus activation of the IRE-1α/XBP-1s pathway, which resulted in activation of the NLRP3 inflammasome- and caspase-1-dependent pyroptosis in HK-2 cells. Inhibition of caspase-1 activity with YVAD, of ER stress with 4-PBA, or of the IRE-1α/XBP-1s pathway with STF-083010 and activation of SIRT1 by specific activator resveratrol or ectopic overexpression significantly mitigated Cd-induced pyroptosis in HK-2 cells

Acknowledgements This study was supported by Grant (no. 21277033) from the national Natural Science Foundation of China; Grant (no. 14DZ2260200, the Project of Shanghai Key Laboratory of Kidney and Blood Purification) from the Scienceand Technology Commission of Shanghai Municipality; Program of China-Sri Lanka Joint Research and Demonstration Center for Water Technology and China-Sri Lanka Joint Center for Education and Research by Chinese Academy of Sciences, China and Grant (no. 15GWZK0202) from the Fourth Round of Three-year Public Health Action Plan of Shanghai. The authors thank Dr. Wusheng Xiao for his critical language editing of this manuscript.

Compliance with ethical standards

Conflict of interest The authors declare no conflict of interest.

References

Benham AM (2012) Protein secretion and the endoplasmic reticulum. Cold Spring Harb Perspect Biol 4(8):a012872. https://doi.org/10.1101/cshperspect.a012872

Bergsbaken T, Cookson BT (2007) Macrophage activation redirects yersinia-infected host cell death from apoptosis to caspase-1-dependent pyroptosis. PLoS Pathog 3(11):e161. https://doi.org/10.1371/journal.ppat.0030161

Bergsbaken T, Fink SL, Cookson BT (2009) Pyroptosis: host cell death and inflammation. Nat Rev Microbiol 7(2):99–109. https://doi.org/10.1038/nrmicro2070

Blander G, Guarente L (2004) The Sir2 family of protein deacetylases. Annu Rev Biochem 73:417–435. https://doi.org/10.1146/annurev.biochem.73.011303.073651

Boonprasert K, Satarug S, Morais C et al (2016) The stress response of human proximal tubule cells to cadmium involves up-regulation of haemoxygenase 1 and metallothionein but not cytochrome P450 enzymes. Toxicol Lett 249:5–14. https://doi.org/10.1016/j.toxlet.2016.02.016

Brunet A, Sweeney LB, Sturgill JF et al (2004) Stress-dependent regulation of FOXO transcription factors by the SIRT1 deacetylase. Science 303(5666):2011–2015. https://doi.org/10.1126/science.1094637

Brzoska MM, Kaminski M, Supernak-Bobko D, Zwierz K, Moniuszko-Jakoniuk J (2003) Changes in the structure and function of the kidney of rats chronically exposed to cadmium. I. Biochemical and histopathological studies. Arch Toxicol 77(6):344–352. https://doi.org/10.1007/s00204-003-0451-1

Burrows JA, Willis LK, Perlmutter DH (2000) Chemical chaperones mediate increased secretion of mutant alpha 1-antitrypsin (alpha 1-AT) Z: a potential pharmacological strategy for prevention of liver injury and emphysema in alpha 1-AT deficiency. Proc Natl Acad Sci USA 97(4):1796–1801 https://doi.org/10.1073/pnas.97.4.1796

Cerqueira DM, Pereira MS, Silva AL, Cunha LD, Zamboni DS (2015) Caspase-1 but not caspase-11 is required for NLRC4-mediated pyroptosis and restriction of infection by flagellated Legionella species in mouse macrophages and in vivo. J Immunol 195(5):2303–2311. https://doi.org/10.4049/jimmunol.1501223

Chen X, Zhu G (2018) The association between dietary cadmium exposure and renal dysfunction—the benchmark dose estimation of reference levels: the ChinaCad study. J Appl Toxicol 38(10):1365–1373. https://doi.org/10.1002/jat.3647

Chen H, Lu Y, Cao Z et al (2016) Cadmium induces NLRP3 inflammasome-dependent pyroptosis in vascular endothelial cells. Toxicol Lett 246:7–16. https://doi.org/10.1016/j.toxlet.2016.01.014

Chen A, Chen Z, Xia Y et al (2018a) Liraglutide attenuates NLRP3 inflammasome-dependent pyroptosis via regulating SIRT1/NOX4/ROS pathway in H9c2 cells. Biochem Biophys Res Commun 499(2):267–272. https://doi.org/10.1016/j.bbrc.2018.03.142

Chen X, Wang Z, Zhu G, Nordberg GF, Ding X, Jin T (2018b) The association between renal tubular dysfunction and zinc level in a

Chinese population environmentally exposed to cadmium. Biol Trace Elem Res 186(1):114–121. https://doi.org/10.1007/s12011-018-1304-3

Ellgaard L, Helenius A (2003) Quality control in the endoplasmic reticulum. Nat Rev Mol Cell Biol 4(3):181–191. https://doi.org/10.1038/nrm1052

Fan Y, Xiao W, Li Z et al (2015) RTN1 mediates progression of kidney disease by inducing ER stress. Nat Commun 6:7841. https://doi.org/10.1038/ncomms8841

Fantuzzi G, Dinarello CA (1999) Interleukin-18 and interleukin-1 beta: two cytokine substrates for ICE (caspase-1). J Clin Immunol 19(1):1–11. https://doi.org/10.1023/A:1020506300324

Faroon O, Ashizawa A, Wright S et al (2012) Toxicological profile for cadmium. Agency for Toxic Substance and Disease Registry (US), Atlanta

Fink SL, Bergsbaken T, Cookson BT (2008) Anthrax lethal toxin and Salmonella elicit the common cell death pathway of caspase-1-dependent pyroptosis via distinct mechanisms. Proc Natl Acad Sci USA 105(11):4312–4317. https://doi.org/10.1073/pnas.0707370105

Fu Y, Wang Y, Du L et al (2013) Resveratrol inhibits ionising irradiation-induced inflammation in MSCs by activating SIRT1 and limiting NLRP-3 inflammasome activation. Int J Mol Sci 14(7):14105–14118. https://doi.org/10.3390/ijms140714105

Ge Z, Diao H, Ji X, Liu Q, Zhang X, Wu Q (2018) Gap junctional intercellular communication and endoplasmic reticulum stress regulate chronic cadmium exposure induced apoptosis in HK-2 cells. Toxicol Lett 288:35–43. https://doi.org/10.1016/j.toxlet.2018.02.013

Gu J, Dai S, Liu Y et al (2018) Activation of Ca(2+)-sensing receptor as a protective pathway to reduce cadmium-induced cytotoxicity in renal proximal tubular cells. Sci Rep 8(1):1092. https://doi.org/10.1038/s41598-018-19327-9

Guo P, Pi H, Xu S et al (2014) Melatonin Improves mitochondrial function by promoting MT1/SIRT1/PGC-1 alpha-dependent mitochondrial biogenesis in cadmium-induced hepatotoxicity in vitro. Toxicol Sci 142(1):182–195. https://doi.org/10.1093/toxsci/kfu164

Guo R, Liu W, Liu B, Zhang B, Li W, Xu Y (2015) SIRT1 suppresses cardiomyocyte apoptosis in diabetic cardiomyopathy: an insight into endoplasmic reticulum stress response mechanism. Int J Cardiol 191:36–45. https://doi.org/10.1016/j.ijcard.2015.04.245

Haigis MC, Sinclair DA (2010) Mammalian sirtuins: biological insights and disease relevance. Annu Rev Pathol 5:253–295. https://doi.org/10.1146/annurev.pathol.4.110807.092250

Hasnain SZ, Lourie R, Das I, Chen AC, McGuckin MA (2012) The interplay between endoplasmic reticulum stress and inflammation. Immunol Cell Biol 90(3):260–270. https://doi.org/10.1038/icb.2011.112

He WT, Wan H, Hu L et al (2015) Gasdermin D is an executor of pyroptosis and required for interleukin-1beta secretion. Cell Res 25(12):1285–1298. https://doi.org/10.1038/cr.2015.139

Huo J, Huang Z, Li R et al (2018) Dietary cadmium exposure assessment in rural areas of Southwest China. PLoS One 13(8):e0201454. https://doi.org/10.1371/journal.pone.0201454

Jarup L, Akesson A (2009) Current status of cadmium as an environmental health problem. Toxicol Appl Pharmacol 238(3):201–208. https://doi.org/10.1016/j.taap.2009.04.020

Kang X, Yang W, Wang R et al (2018) Sirtuin-1 (SIRT1) stimulates growth-plate chondrogenesis by attenuating the PERK-eIF-2alpha-CHOP pathway in the unfolded protein response. J Biol Chem 293(22):8614–8625. https://doi.org/10.1074/jbc.M117.809822

Kato H, Nakajima S, Saito Y, Takahashi S, Katoh R, Kitamura M (2012) mTORC1 serves ER stress-triggered apoptosis via selective activation of the IRE1-JNK pathway. Cell Death Differ 19(2):310–320. https://doi.org/10.1038/cdd.2011.98

Klaassen CD, Liu J, Diwan BA (2009) Metallothionein protection of cadmium toxicity. Toxicol Appl Pharmacol 238(3):215–220. https://doi.org/10.1016/j.taap.2009.03.026

Kriss CL, Pinilla-Ibarz JA, Mailloux AW et al (2012) Overexpression of TCL1 activates the endoplasmic reticulum stress response: a novel mechanism of leukemic progression in mice. Blood 120(5):1027–1038. https://doi.org/10.1182/blood-2011-11-394346

Lebeaupin C, Proics E, de Bieville CH et al (2015) ER stress induces NLRP3 inflammasome activation and hepatocyte death. Cell Death Dis 6:e1879. https://doi.org/10.1038/cddis.2015.248

Lee AH, Iwakoshi NN, Glimcher LH (2003) XBP-1 regulates a subset of endoplasmic reticulum resident chaperone genes in the unfolded protein response. Mol Cell Biol 23(21):7448–7459. https://doi.org/10.1128/MCB.23.21.7448-7459.2003

Lerner AG, Upton JP, Praveen PV et al (2012) IRE1alpha induces thioredoxin-interacting protein to activate the NLRP3 inflammasome and promote programmed cell death under irremediable ER stress. Cell Metab 16(2):250–264. https://doi.org/10.1016/j.cmet.2012.07.007

Li Y, Xu S, Giles A et al (2011) Hepatic overexpression of SIRT1 in mice attenuates endoplasmic reticulum stress and insulin resistance in the liver. FASEB J 25(5):1664–1679. https://doi.org/10.1096/fj.10-173492

Li PC, Wang BR, Li CC et al (2018) Seawater inhalation induces acute lung injury via ROS generation and the endoplasmic reticulum stress pathway. Int J Mol Med 41(5):2505–2516. https://doi.org/10.3892/ijmm.2018.3486

Liu Y, Liu J, Habeebu SM, Waalkes MP, Klaassen CD (2000) Metallothionein-I/II null mice are sensitive to chronic oral cadmium-induced nephrotoxicity. Toxicol Sci 57(1):167–176. https://doi.org/10.1093/toxsci/57.1.167

Liu F, Li ZF, Wang ZY, Wang L (2016) Role of subcellular calcium redistribution in regulating apoptosis and autophagy in cadmium-exposed primary rat proximal tubular cells. J Inorg Biochem 164:99–109. https://doi.org/10.1016/j.jinorgbio.2016.09.005

Liu YG, Chen JK, Zhang ZT et al (2017) NLRP3 inflammasome activation mediates radiation-induced pyroptosis in bone marrow-derived macrophages. Cell Death Dis 8(2):e2579. https://doi.org/10.1038/cddis.2016.460

Lu A, Magupalli VG, Ruan J et al (2014) Unified polymerization mechanism for the assembly of ASC-dependent inflammasomes. Cell 156(6):1193–1206. https://doi.org/10.1016/j.cell.2014.02.008

Lu Y, Xu S, Chen H et al (2016) CdSe/ZnS quantum dots induce hepatocyte pyroptosis and liver inflammation via NLRP3 inflammasome activation. Biomaterials 90:27–39. https://doi.org/10.1016/j.biomaterials.2016.03.003

Luo B, Lin Y, Jiang S et al (2016) Endoplasmic reticulum stress eIF2alpha-ATF4 pathway-mediated cyclooxygenase-2 induction regulates cadmium-induced autophagy in kidney. Cell Death Dis 7(6):e2251. https://doi.org/10.1038/cddis.2016.78

Ma Q (2013) Role of nrf2 in oxidative stress and toxicity. Annu Rev Pharmacol Toxicol 53:401–426. https://doi.org/10.1146/annurev-pharmtox-011112-140320

Morigi M, Perico L, Benigni A (2018) Sirtuins in renal health and disease. J Am Soc Nephrol 29(7):1799–1809. https://doi.org/10.1681/asn.2017111218

Olszowski T, Baranowska-Bosiacka I, Gutowska I, Chlubek D (2012) Pro-inflammatory properties of cadmium. Acta Biochim Pol 59(4):475–482

Oslowski CM, Hara T, O'Sullivan-Murphy B et al (2012) Thioredoxin-interacting protein mediates ER stress-induced beta cell death through initiation of the inflammasome. Cell Metab 16(2):265–273. https://doi.org/10.1016/j.cmet.2012.07.005

Papandreou I, Denko NC, Olson M et al (2011) Identification of an Ire1alpha endonuclease specific inhibitor with cytotoxic activity

against human multiple myeloma. Blood 117(4):1311–1314. https://doi.org/10.1182/blood-2010-08-303099
Prola A, Pires Da Silva J, Guilbert A et al (2017) SIRT1 protects the heart from ER stress-induced cell death through eIF2alpha deacetylation. Cell Death Differ 24(2):343–356. https://doi.org/10.1038/cdd.2016.138
Ron D, Walter P (2007) Signal integration in the endoplasmic reticulum unfolded protein response. Nat Rev Mol Cell Biol 8(7):519–529. https://doi.org/10.1038/nrm2199
Sabolic I, Breljak D, Skarica M, Herak-Kramberger CM (2010) Role of metallothionein in cadmium traffic and toxicity in kidneys and other mammalian organs. Biometals 23(5):897–926. https://doi.org/10.1007/s10534-010-9351-z
Satarug S (2018) Dietary cadmium intake and its effects on kidneys. Toxics https://doi.org/10.3390/toxics6010015
Schroder M (2008) Endoplasmic reticulum stress responses. Cell Mol Life Sci 65(6):862–894. https://doi.org/10.1007/s00018-007-7383-5
Schroder K, Tschopp J (2010) The inflammasomes. Cell 140(6):821–832. https://doi.org/10.1016/j.cell.2010.01.040
Shi J, Zhao Y, Wang K et al (2015) Cleavage of GSDMD by inflammatory caspases determines pyroptotic cell death. Nature 526(7575):660–665. https://doi.org/10.1038/nature15514
Simard JC, Vallieres F, de Liz R, Lavastre V, Girard D (2015) Silver nanoparticles induce degradation of the endoplasmic reticulum stress sensor activating transcription factor-6 leading to activation of the NLRP-3 inflammasome. J Biol Chem 290(9):5926–5939. https://doi.org/10.1074/jbc.M114.610899
Sui DM, Xie Q, Yi WJ et al (2016) Resveratrol protects against sepsis-associated encephalopathy and inhibits the NLRP3/IL-1beta axis in microglia. Mediat Inflamm 2016:1045657. https://doi.org/10.1155/2016/1045657
Takahashi M (2014) NLRP3 inflammasome as a novel player in myocardial infarction. Int Heart J 55(2):101–105. https://doi.org/10.1536/ihj.13-388
Thijssen S, Lambrichts I, Maringwa J, Van Kerkhove E (2007a) Changes in expression of fibrotic markers and histopathological alterations in kidneys of mice chronically exposed to low and high Cd doses. Toxicology 238(2–3):200–210. https://doi.org/10.1016/j.tox.2007.06.087
Thijssen S, Maringwa J, Faes C, Lambrichts I, Van Kerkhove E (2007b) Chronic exposure of mice to environmentally relevant, low doses of cadmium leads to early renal damage, not predicted by blood or urine cadmium levels. Toxicology 229(1–2):145–156. https://doi.org/10.1016/j.tox.2006.10.011
Vaziri H, Dessain SK, Ng Eaton E et al (2001) hSIR2(SIRT1) functions as an NAD-dependent p53 deacetylase. Cell 107(2):149–159. https://doi.org/10.1016/S0092-8674(01)00527-X
Wang FM, Chen YJ, Ouyang HJ (2011a) Regulation of unfolded protein response modulator XBP1s by acetylation and deacetylation. Biochem J 433(1):245–252. https://doi.org/10.1042/bj20101293
Wang FM, Galson DL, Roodman GD, Ouyang H (2011b) Resveratrol triggers the pro-apoptotic endoplasmic reticulum stress response and represses pro-survival XBP1 signaling in human multiple myeloma cells. Exp Hematol 39(10):999–1006. https://doi.org/10.1016/j.exphem.2011.06.007
Wilmes A, Crean D, Aydin S, Pfaller W, Jennings P, Leonard MO (2011) Identification and dissection of the Nrf2 mediated oxidative stress pathway in human renal proximal tubule toxicity. Toxicol In Vitro 25(3):613–622. https://doi.org/10.1016/j.tiv.2010.12.009
Wu KC, Liu JJ, Klaassen CD (2012) Nrf2 activation prevents cadmium-induced acute liver injury. Toxicol Appl Pharmacol 263(1):14–20. https://doi.org/10.1016/j.taap.2012.05.017
Xiao W, Sarsour EH, Wagner BA et al (2016) Succinate dehydrogenase activity regulates PCB3-quinone-induced metabolic oxidative stress and toxicity in HaCaT human keratinocytes. Arch Toxicol 90(2):319–332. https://doi.org/10.1007/s00204-014-1407-3
Xiao W, Wang RS, Handy DE, Loscalzo J (2018) NAD(H) and NADP(H) redox couples and cellular energy metabolism. Antioxid Redox Signal 28(3):251–272. https://doi.org/10.1089/ars.2017.7216
Xu C, Bailly-Maitre B, Reed JC (2005) Endoplasmic reticulum stress: cell life and death decisions. J Clin Investig 115(10):2656–2664. https://doi.org/10.1172/jci26373
Yam GH, Gaplovska-Kysela K, Zuber C, Roth J (2007) Sodium 4-phenylbutyrate acts as a chemical chaperone on misfolded myocilin to rescue cells from endoplasmic reticulum stress and apoptosis. Investig Ophthalmol Vis Sci 48(4):1683–1690. https://doi.org/10.1167/iovs.06-0943
Yang SJ, Lim Y (2014) Resveratrol ameliorates hepatic metaflammation and inhibits NLRP3 inflammasome activation. Metabolism 63(5):693–701. https://doi.org/10.1016/j.metabol.2014.02.003
Yang H, Shu Y (2015) Cadmium transporters in the kidney and cadmium-induced nephrotoxicity. Int J Mol Sci 16(1):1484–1494. https://doi.org/10.3390/ijms16011484
Yang JR, Yao FH, Zhang JG et al (2014) Ischemia-reperfusion induces renal tubule pyroptosis via the CHOP-caspase-11 pathway. Am J Physiol Ren Physiol 306(1):F75–F84. https://doi.org/10.1152/ajprenal.00117.2013
Yokouchi M, Hiramatsu N, Hayakawa K et al (2007) Atypical, bidirectional regulation of cadmium-induced apoptosis via distinct signaling of unfolded protein response. Cell Death Differ 14(8):1467–1474. https://doi.org/10.1038/sj.cdd.4402154
Zeng X, Jin T, Zhou Y, Nordberg GF (2003) Changes of serum sex hormone levels and MT mRNA expression in rats orally exposed to cadmium. Toxicol 186(1–2):109–118. https://doi.org/10.1016/S0300-483X(02)00725-4
Zhang C, Liang Y, Lei L et al (2013) Hypermethylations of RASAL1 and KLOTHO is associated with renal dysfunction in a Chinese population environmentally exposed to cadmium. Toxicol Appl Pharmacol 271(1):78–85. https://doi.org/10.1016/j.taap.2013.04.025
Zhang Y, Tao X, Yin L et al (2017) Protective effects of dioscin against cisplatin-induced nephrotoxicity via the microRNA-34a/sirtuin 1 signalling pathway. Br J Pharmacol 174(15):2512–2527. https://doi.org/10.1111/bph.13862
Zheng X, Xu F, Liang H et al (2017) SIRT1/HSF1/HSP pathway is essential for exenatide-alleviated, lipid-induced hepatic endoplasmic reticulum stress. Hepatology 66(3):809–824. https://doi.org/10.1002/hep.29238